3D Printing Technologies in Metallic Implants: A Thematic Review on the Techniques and Procedures

Shokouh Attarilar[1,2], Mahmoud Ebrahimi[3], Faramarz Djavanroodi[4,5], Yuanfei Fu[6], Liqiang Wang[2]*, Junlin Yang[1]*

[1]Department of Pediatric Orthopaedics, Xinhua Hospital Affiliated to Shanghai Jiao Tong University, School of Medicine, Shanghai, China
[2]State Key Laboratory of Metal Matrix Composites, School of Material Science and Engineering, Shanghai Jiao Tong University, Shanghai, China
[3]National Engineering Research Center of Light Alloy Net Forming, School of Materials Science and Engineering, Shanghai Jiao Tong University, Shanghai, China
[4]Department of Mechanical Engineering, College of Engineering, Prince Mohammad Bin Fahd University, Al Khobar, KSA
[5]Department of Mechanical Engineering, Imperial College London, London, UK
[6]Ninth People's Hospital, School of Medicine, Shanghai Jiao Tong University, Shanghai 200011, China

Abstract: Additive manufacturing (AM) is among the most attractive methods to produce implants, the processes are very swift and it can be precisely controlled to meet patient's requirement since they can be produced in exact shape, dimension, and even texture of different living tissues. Until now, lots of methods have emerged and used in this field with diverse characteristics. This review aims to comprehensively discuss 3D printing (3DP) technologies to manufacture metallic implants, especially on techniques and procedures. Various technologies based on their main properties are categorized, the effecting parameters are introduced, and the history of AM technology is briefly analyzed. Subsequently, the utilization of these AM-manufactured components in medicine along with their effectual variables is discussed, and special attention is paid on to the production of porous scaffolds, taking pore size, density, etc., into consideration. Finally, 3DP of the popular metallic systems in medical applications such as titanium, Ti6Al4V, cobalt-chromium alloys, and shape memory alloys are studied. In general, AM manufactured implants need to comply with important requirements such as biocompatibility, suitable mechanical properties (strength and elastic modulus), surface conditions, custom-built designs, fast production, etc. This review aims to introduce the AM technologies in implant applications and find new ways to design more sophisticated methods and compatible implants that mimic the desired tissue functions.

Keywords: Additive manufacturing; 3D printing techniques; Biometals; Implants; Porous scaffolds

*Correspondence to: Liqiang Wang, State Key Laboratory of Metal Matrix Composites, School of Material Science and Engineering, Shanghai Jiao Tong University, Shanghai, China; wang_liqiang@sjtu.edu.cn. Junlin Yang, Department of Pediatric Orthopaedics, Xinhua Hospital Affiliated to Shanghai Jiao Tong University, School of Medicine, Shanghai, China; yjunlin@126.com

Citation: Attarilar S, Ebrahimi M, Djavanroodi F, *et al*., 2021, 3D Printing Technologies in Metallic Implants: A Thematic Review on the Techniques and Procedures. *Int J Bioprint,* 7(1): 306. http://doi.org/10.18063/ijb.v7i1.306

1. Introduction

As the world's elderly population grows, the need for medical implants is rapidly growing. It is expected that the number of people aged 65 or above will increase to about 20% of the world population by 2050[1]. These elderly patients and other patients with bone fracture and failures need special cares, specifically those associated with rapid healing time, fast preparation of implants, and custom-built implants that are tailored to patients' fracture conditions. Furthermore, avoiding possible subsidiary issues arise from low-quality designs, stress-shielding effects, and infections. The traditionally manufactured implants have a lot of limitations, such as a time-consuming production process, low capability in

producing complex shapes, and difficulty to manufacture the custom-built designs. Hence, advance procedures are highly required to meet various demands from patients and healthcare market.

Three-dimensional printing (3DP) is an evolutionary technology and a branch of additive manufacturing (AM) methods that cover a range of applications in modern industries, including manufacturing of computer components, electricity, machinery, and digital control devices[2]. According to the AM principles and the use of special 3D bioprinters, human organs can be artificially produced[3] in the future, and the realization of this goal will be accompanied by a revolution in the healthcare system. These 3DP techniques have great potentials in producing porous and complex-shaped materials and components with very intricate internal structures. Therefore, 3DP technology enables fabrication of hierarchical materials with porous structure and mechanical properties (strength and elastic Young's modulus) very similar to natural bone and inhibits stress-shield effect in bone implants[4-6]. Moreover, 3DP technologies have some other advantages, including the ability in mass production, economic efficiency, low cost, repeatability, and shorter time to market[2]. In addition, 3D technology together with computer-aided design (CAD) technique[7] can be used in the production of completely patient-specific implants[8,9]. 3DP method developed rapidly and a variety of new techniques with many advantages were devised to cure the previous limitations. The first description about 3DP dates back to 1981 when Dr. Hideo Kodama fabricated a device that uses ultraviolet (UV) lights to harden polymers and create solid objects[10]. Although it was not commercialized, it was the first step to the conception of stereolithography (SLA) technique in 1983. Later, Charles Hull invented the first SLA machine[11]. In 1987, a selective laser sintering (SLS) process was patented, and the first commercial rapid prototyping printer entitled SLA-1 was sold 1 year later. Subsequently, fused deposition modeling (FDM) and laser AM (LAM) were introduced. Following the introduction of newly developed 3D printing techniques, Israeli scientists made a successful achievement in the fabrication of an entire heart with human cells in 2019[12], **Figure 1** schematically represents the 3DP history.

The 3DP process is performed sequentially based on the following steps: First, using the digital design software (SolidWorks, AutoCAD, Autodesk, etc.), 3D digital scanners, or other applications, the digital virtual version of the desired object is generated. Then, the 3D digital model is transformed into SLA or standard tessellation language (.STL) file format. The .STL file involves numerous triangulated facets that demonstrate the exact spatial coordinates (xyz) information of 3D model surfaces. A large

Figure 1. Timeline of 3D printing technologies.

number of triangles means more data points and higher resolutions. Third, by utilizing particular slicer software in

the 3D printer machine, the .STL file is converted into G file through slicing the designed model into 2D horizontal cross-section arrays in a size range of 25 – 100 μm. Then, the first layer of the 3D object is formed by the x-y movement of the printer head. Finally, the rest of the object was created through the incessant movement of the printer head in the z-direction; hence, the desired morphology can be deposited layer by layer on the first basal sheet as a substrate[13]. However, this printing procedure is highly dependent on the 3DP machine. The general production procedure is represented schematically in **Figure 2**.

3DP can utilize various types of materials such as ABS plastic, PLA, polyamide (nylon), glass filled polyamide, SLA materials (epoxy resins), silver, titanium, steel, wax, photopolymers and polycarbonate, cells, hydrogels, etc. Among these materials, metallic materials are of great importance in the biomedical field. The metallic materials used in AM technology must adhere to two crucial requirements: First, they must have good weldability to prevent crack formation during solidification; second, the raw metallic material should be prepared in the form of spherical powder with a size of tens micrometers range to satisfy the acceptable packing density and homogeneity requirements of the AM manufactured part. About 50 metallic alloys can be used in AM manufacturing, and they are mostly Ti-, Ni-, Al-, and Cu-based alloys, tool steels, stainless steels, Co-Cr alloys, and some precious and refractory metals[14]. More than 80% of all used implants in medicine are metallic ones and they are categorized into two different groups: Bio-degradable and non-degradable metallic implants[1]. Biodegradable metals include iron, magnesium, zinc, and calcium. Considering the excellent advantages of 3DP, this technology will have a great impact and an increase of its applications, especially in the biomedical field, is expected in near future. Therefore, a comprehensive understanding of the recent methods and techniques opens up a new horizon for optimum design and fabrication of more advanced materials for implant

applications. This thematic review provides some insights into the realization of this purpose.

2. 3DP process techniques

ASTM Committees grouped different types of AM into seven main categories based depending on the material addition method and working procedure (**Figure 3**). In fact, each of these seven main methods has its pros and cons according to the main objective of fabricating a 3D printed specimen. A right method is essential and it is generally selected according to the following parameters: Material type (plastic, metal alloys, ceramics, sand, and wax), material state (liquid, powder, wire, etc.), material compatibility, and its availability, consolidation type (polymerizing, laser melting or sintering, fusing, UV curing, etc.), desired feature size, resolution, throughput, and speed[13]. In biomedical 3DP extrusion[15], thermal inkjet and laser-assisted techniques are commonly used. The most common techniques for metal 3DP are powder bed fusion or melting methods, among which the selective laser melting (SLM) and electron beam melting (EBM) are very popular and they are the most widely used 3DP methods in the world. Direct energy deposition uses metal feedstock and a laser to fabricate parts. Vat photopolymerization selectively cures a vat of liquid photopolymer through targeted light-activated polymerization to produce 3D printed components. All the various methods are well-classified and represented in **Figure 3** and the detailed information about each of the methods is included in following sections.

2.1. Vat photopolymerization

SLA is the first patented and commercialized AM process which uses a vat photopolymerization technique, and the 3D objects are generated in this process by selectively curing a vat of liquid photopolymer through targeted light-activated polymerization. The SLA, digital light processing (DLP), continuous, direct light processing
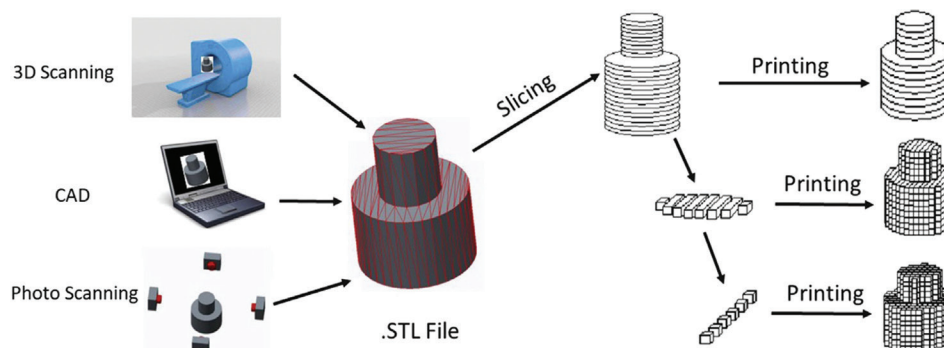

Figure 2. Schematic representation of the 3D printing process (Reprinted from 3D *Printing Technology* in *Nanomedicine*, 1ˢᵗ edition, Ashish, Ahmad N, Gopinath P, *et al*, 3D *Printing* in Medicine: Current Challenges and Potential Applications, pp 1-22, Copyright (2019), with permission from Elsevier)[13].
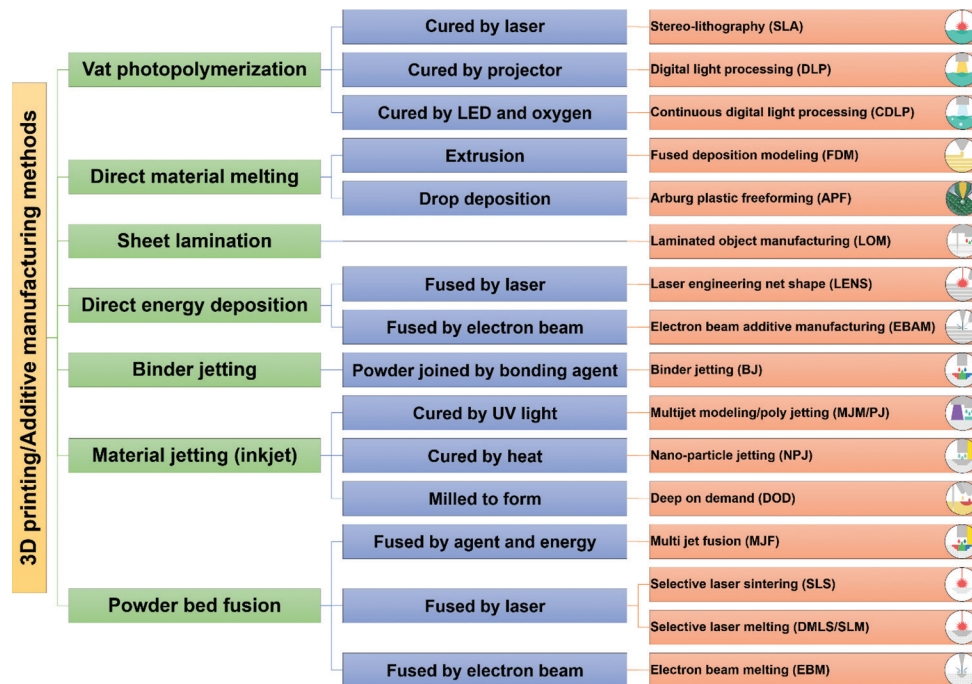
Figure 3. An overview of the most important additive manufacturing technologies.

(CDLP), and bio-plotters use vat photopolymerization technology[13]. In the photopolymerization technology, the primarily used materials are liquid, radiation-curable resins, or photopolymers such as polyimides, elastomers, pure polymer resin, composite resins, supramolecular polymers, graphene, and ceramic slurry + resins. Mostly, UV wavelength and some light systems can be used for radiation of photopolymers. Radiation on photopolymer materials leads to a chemical reaction, known as photopolymerization, that solidifies the materials. Photopolymers were first used in 1960s and later applied in glossy coatings of papers and cardboards, dentistry, etc. In the middle of the 1980s, Charles Hull fabricated a 3D solid part by laser scanning over a UV-curable material and cured one layer over a previous layer, representing the very first step toward SLA technology[16]. In this regard, **Figure 4** shows a schematic of the SLA vat-based method. Vat-based AM methods have numerous advantages, including excellent print resolution, good surface finishing, high efficiency, versatility, and superior printing accuracy.

In SLA technique, the production process starts with the deposition of photopolymer material as a first layer on the build platform by utilizing a recoating mechanism. The desired pattern produced by a UV laser raster on the resin surface and leads to the cross-linking of the liquid photopolymer into solid form. The subsequent layers are built by recoating a new layer and its patterning with a UV beam. The controlling parameters in this technique are scanning speed, exposure time, laser power, material composition, and photoinitiator[17]. Three different
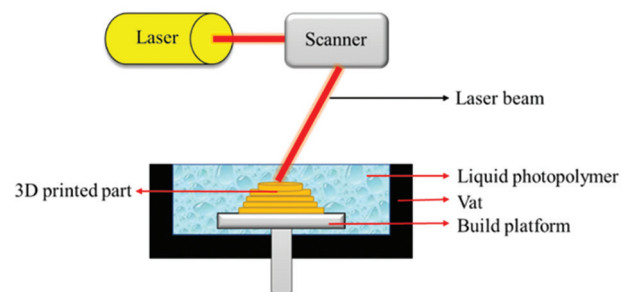

Figure 4. A schematic diagram of the stereolithography vat-based technique.

mechanisms are used in vat-based photopolymerization methods, including vector scan SL, mask projection, and two-photon approach (**Figure 5**). Among different influencing parameters, laser wavelength has a key role in regulating laser power. Each laser type uses a specific wavelength; for example, in the SLA-250 device, a helium-cadmium (He-Cd) laser type with 325 nm wavelength is used; other SLA devices from 3D Systems have Nd-YVO4 lasers with 1062 nm wavelengths (near-infrared); a high power titanium-sapphire laser with 790 nm wavelength is used in a 2p-VP two-photon vat-based device[16].

Another popular vat-based method is mask-projection vat photopolymerization (MPVP), also known as DLP, that can achieve resolutions in the range of 30 μm. In DLP method instead of laser beam utilization in the two-photon and vector scan systems, a large radiation beam is patterned by the utilization of another device such as Digital Micromirror Device™ (DMD) a large radiation

beam is patterned by the utilization of another device such as Digital Micromirror Device™. In the two-photon approach, the photopolymerization process is implemented at the intersecting point of two laser beams[16].

2.2. Powder-bed fusion

In powder-bed 3DP techniques, a thermal source is utilized to selectively melt or fuse the substances (wax, metal, nylon, polymer, plastic, ceramic, composite) which are held in a tray and the melt or fused materials are then sequentially printed in a layer-by-layer manner. Several examples of the printing methods following the power-bed 3D printing include EBM, SLS, polymer laser sintering, direct metal laser sintering and SLM[18].

The basic of laser powder-bed fusion is shown in **Figure 6A**. A laser beam scans the target location of the powder bed with specified speed and energy to convert the powder fusion into solid form, under full melting SLS (SLM) or partial melting SLS condition. According to the

defined layer thickness, the powder bed is lowered, and the fresh layer of powder is prepared after the completion of previous layers. This method was repeated several times to complete the fabrication[19,20].

(1) SLM method

Being one of the most popular prototyping methods, the SLM method uses high power-density laser to fuse metal or metallic alloy powders to produce AlSi10Mg parts[22], martensitic high strength steel[23], and Al–Scalloy[24]. The production of 3D part by SLM involves a series of steps from digital design data preparation to the removal of the completed part from the building platform. First, to generate the slice data of each layer for laser scanning, SLA (STL) files must be produced by software such as Materialise Magics. Then, the CAD data are uploaded to the SLM machine. The building procedure starts with laying the first thin layer of metal powder on a tray. Soon after the powder is laid, a laser beam with a high energy-
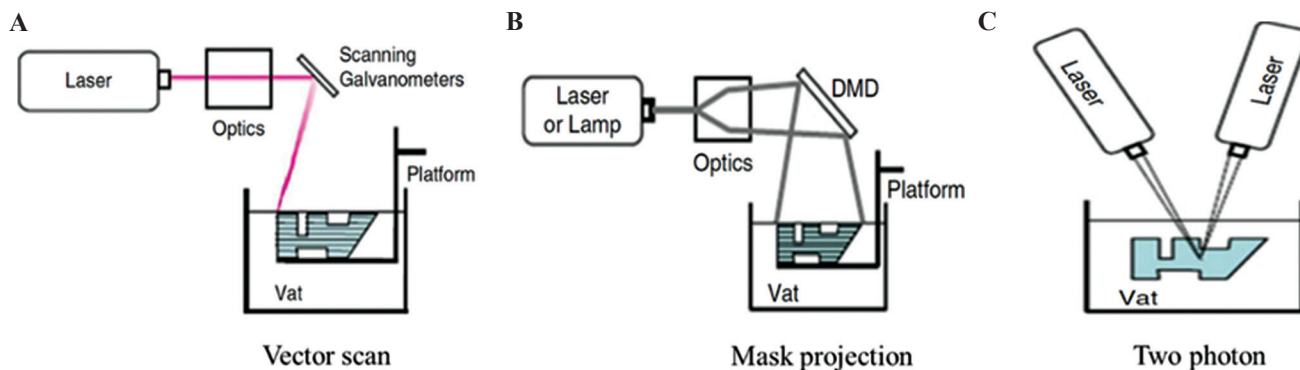

Figure 5. Various photopolymerization mechanisms in vat-based methods. (A) Vector scan SL. (B) Mask projection. (C) Two-photon approaches.
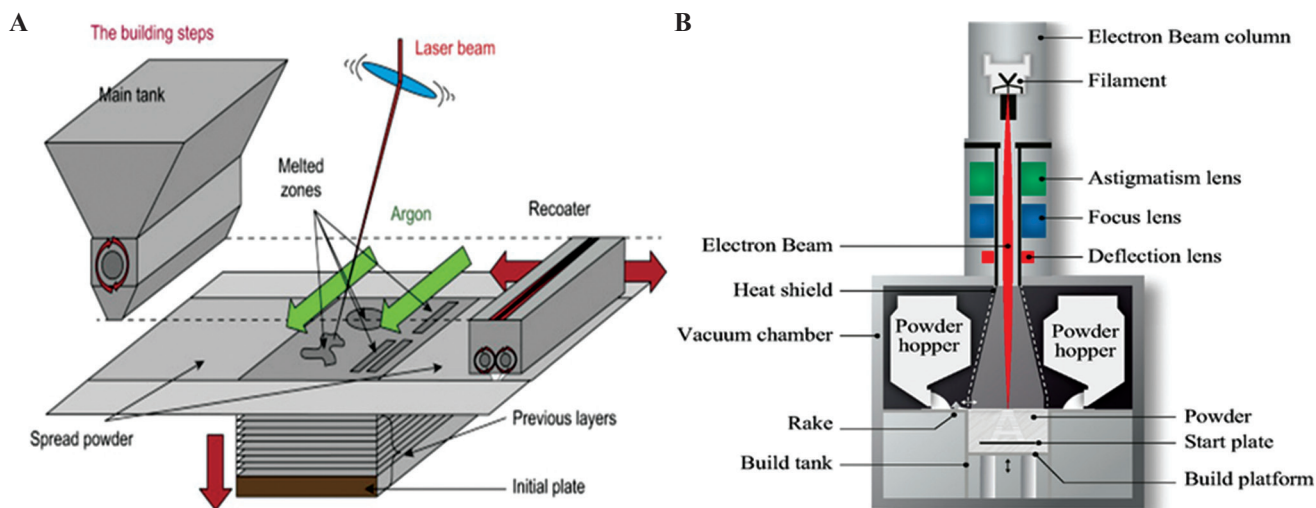

Figure 6. (A) Schematic presentation of the laser-based powder-bed fusion process. (B) Main components of an electron beam melting technique (Reprinted from *Additive Manufacturing*, Volume 19, Galati M and Luliano L, A literature review of powder-based electron beam melting focusing on numerical simulations, pp 1-20, Copyright (2018), with permission from Elsevier)[21].

density beam is utilized to melt and fuse the preferred regions according to CAD data. After the completion of the first layer, the building platform is lowered, and the subsequent layer of powder is deposited on the previous layer before the laser beam begins to scan a new layer. This procedure is repeated several times until the entire 3D part is fabricated. The completed 3D part is then removed from the platform manually or by electrical discharge machining (EDM) and the loose powders removed from the surface[25]. **Figure 7** shows the schematic presentation of the processing steps in the SLM technique.

The key process variables of the SLM technique, such as scanning speed, laser power, hatch spacing, and layer thickness, must be accurately regulated. Furthermore, some important physical aspects should be considered, including thermal fluctuation in the material that will lead to crack initiation and failure, the balling issue that intervenes in continuous melt formation, and the absorptivity of material toward laser irradiation[25].

(2) EBM method

The EBM method, as one of the layer-by-layer techniques, is among the most used AM techniques. It can be used to produce high-quality metal and metallic alloys parts[27-29] and the near net shape metallic samples with complex geometries[30]. In this method, the structures are made by selective melting of discrete powder layers through electron-beam gun under the vacuum condition. The melting process is engendered by the energy emission from the electron beam of a tungsten filament which consists of two magnetic coils for controlling the beam position and diameter and the adjustment of focusing and defocusing conditions[31]; **Figure 6B** demonstrates a schematic presentation of the EMB device. Furthermore, **Figure 8** represents the EBM chamber (**Figure 8A**) and the EBM process steps (**Figure 8B**). In the EBM technique, each slice is categorized in two distinct regions named contours and squares. First, the contour region which acts as an interface between the part and the surrounding powders is produced. Then, the square parts of the inner region of these boundary and contour zones are fabricated by EBM. Performing the EBM process in the vacuum condition prevents impurity and contamination that leads to the formation of high-quality parts with good mechanical properties[32,33]. After the complete fabrication of a 3D printed object, the part is kept inside the chamber for cooling. Then, excess powders are removed from the part, and because of the relatively rough surface of the EBM parts[34,35], they are subject to final surface treatments through milling, turning, polishing, and grinding devices[36].

2.3. Binder jetting

The binder jetting-based techniques, also known as the direct 3DP, use the inkjet printing system. Specifically, the printer head in this system not only moves in the x-y plane as the conventional state but also runs in the
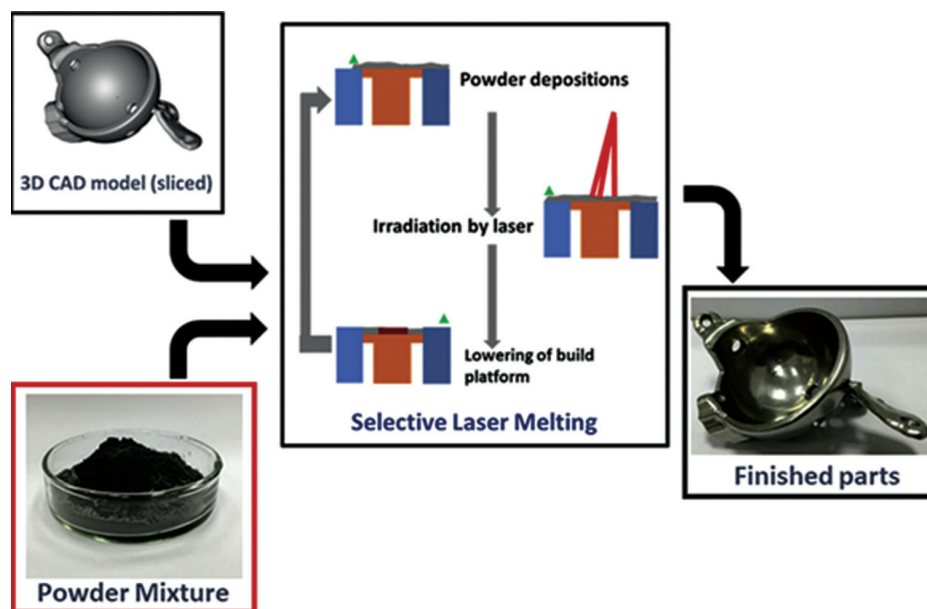

Figure 7. Schematic representation of the processing steps in the selective laser melting (Reprinted from International Journal of Refractory Metals and Hard Materials, Volume 77, Sing SL, Wiria F E and Yeong WY, Selective laser melting of titanium alloy with 50 wt% tantalum: Effect of laser process parameters on part quality, pp 120-127, Copyright (2018), with permission from Elsevier)[26]. The powder mixture is added into chamber and then the laser scanned and fused the powders according to the sliced computer-aided design data. Subsequently, the cycle of powder deposition, laser irradiation, and lowering the tray is repeated until the entire 3D part is produced.
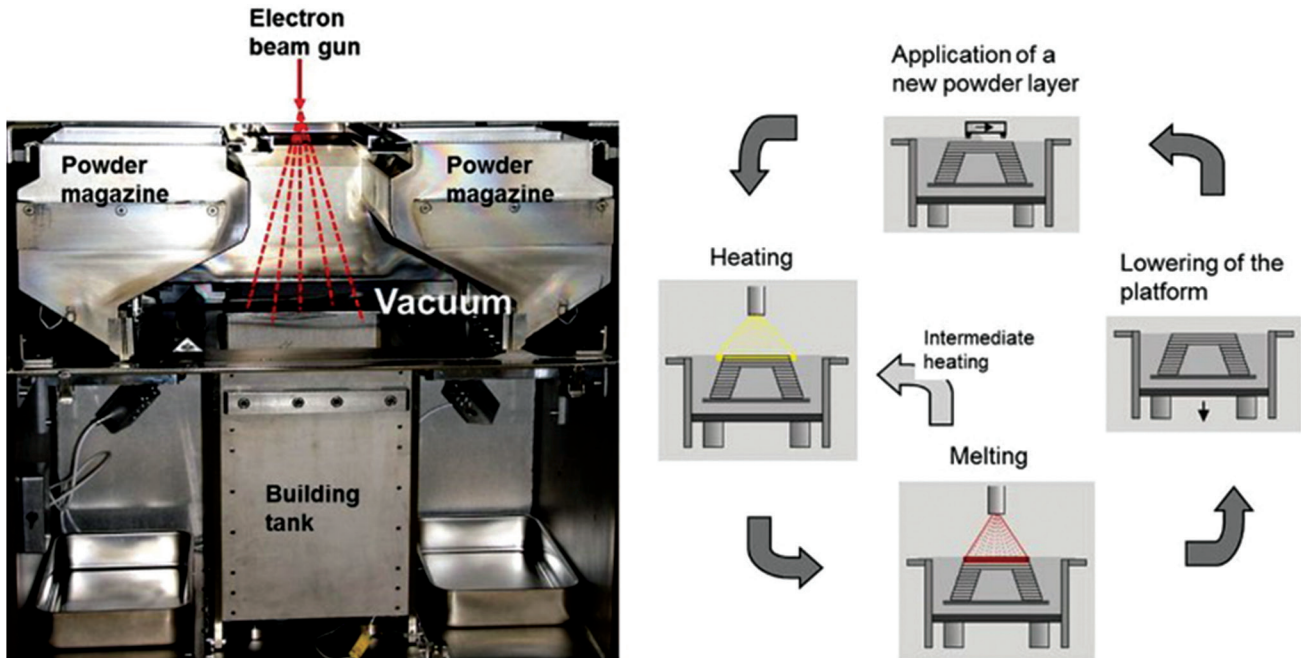
Figure 8. Selective electron beam melting technique. (A) Process chamber. (B) Four-step cyclic process for building layer-by-layer final 3D part[37]

z-direction using the height-adjustable platform. This type of movement in the coordinate system is suitable for simultaneous printing of the objects in all directions[38]. This system is similar to that of the powder-bed fusion, in which a substance layer is deposited over the bed and then leveled with the roller. Then, the multichannel print head, according to the coordinate system and parameters of the CAD file, dispenses the droplets of binder material onto the powder bed before the ultimate binding of powder particles. After finishing the first layer, the device piston lowered the powder bed and the deposition of the next layer began[39]. **Figure 9** shows the schematic presentation of binder jetting technology in 3DP.

2.4. Material jetting

Material jetting or multijet modeling (MJM) is one of the photopolymer-based injecting systems which build the whole 3D object layer-by-layer through multiple nozzles. The chemical basis that is similar with vat photopolymerization is also utilized in material jetting technique, but the liquid material is not kept inside the vat container. Furthermore, similar to the inkjet printing technology, the printer head of this method distributes the polymeric substance over the substrate which is subsequently cured with UV light. Afterward, the finished layer of the object is gradually lowered to let the upper layers to be built[41]. Along with the photopolymeric substance, some kind of jelly or wax material was added to support the printing procedure[42]. The impressive characteristic of these MJM methods is
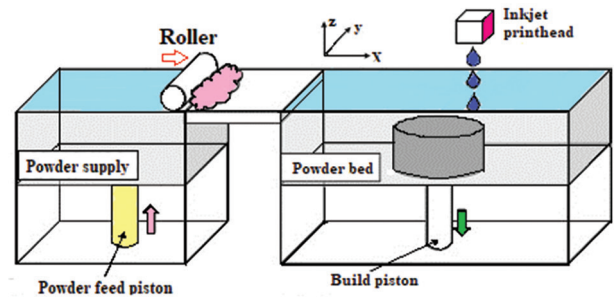

Figure 9. The binder jetting technology (Reprinted from *Additive Manufacturing*, Zhang Y, Jarosinski W, Jung YG, *et al*, Additive manufacturing processes and equipment, pp. 39 –51, Copyright (2018), with permission from Elsevier)[40].

their ability to simultaneously deliver up to fourteen types of materials; therefore, this kind of method can build a 3D object with multiple properties such as various colors, hard and soft type of plastics for different regions of an object, and different morphological and elastomeric conditions[43]. **Figure 10** represents the schematic illustration of this method.

2.5. Material extrusion

Material extrusion method utilizes special heating nozzles and pneumatic or mechanical facilities and through them the collected 3D printing material in the chamber is dispensed. These extrusion-based methods are favorites of both industrial manufacturers and researchers since they are easy to use and economical. This method can
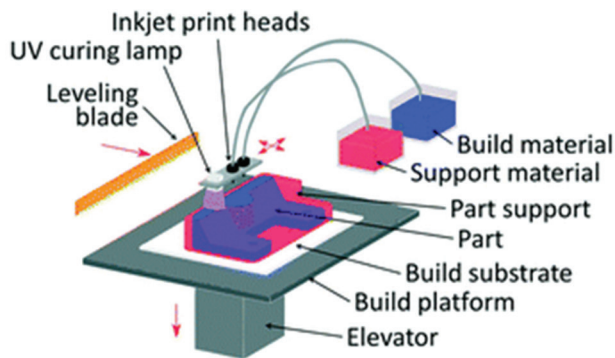
Figure 10. Schematic illustration of material jetting or multijet modelling (Reproduced by permission of The Royal Society of Chemistry)[44].

be used in two distinctive ways along with material melting (precise extrusion deposition[45], precise extrusion manufacturing[46], multiphase jet solidification[47], and fused deposition modeling[48]) and without material melting (direct-write assembly[49], solvent-based extrusion free-forming[50], 3D bioplotting, robocasting[51], pressure-assisted microsyringe[52], and low temperature deposition manufacturing)[53]. FDM is the most well-known among these versatile material extrusion techniques. In FDM, the material (usually a thermoplastic or composite) is extruded by special nozzle systems which consist of, for instance, heated and digitally controllable nozzles that can move in all three directions. After the heating or melting procedure, the material or substance that flows through the nozzle equipped with a temperature control system will rapidly solidify upon its first contact with the air. After the deposition of the first layer, the stage is lowered to continue and complete the layer-by-layer formation of the 3D object[39,44].

2.6. Sheet lamination

The 3DP methods, similar to laminated object manufacturing (LOM), are categorized in sheet lamination group. This type of method fabricates a 3D object that involves a layer-by-layer lamination of a sheet material such as metal, plastic, and paper. Initially, the sheet material which is coated with an adhesive substance is located on the stage; subsequently, the sheet is traced using a beam of laser or a razor, and its cross-section is cut based on the 3D CAD model[54,55]. Second, the excess material that is not needed anymore is removed by the laser. Following this procedure, the stage is lowered to deposit the next layers on the previous ones. Finally, these steps are repeated until a 3D object is made. **Figure 11** shows the schematic illustration of the LOM process. The LOM-fabricated objects have several benefits compared to other AM-produced objects, including (i) higher resistance to deformation and distortions due to their low internal tensions, (ii) lower
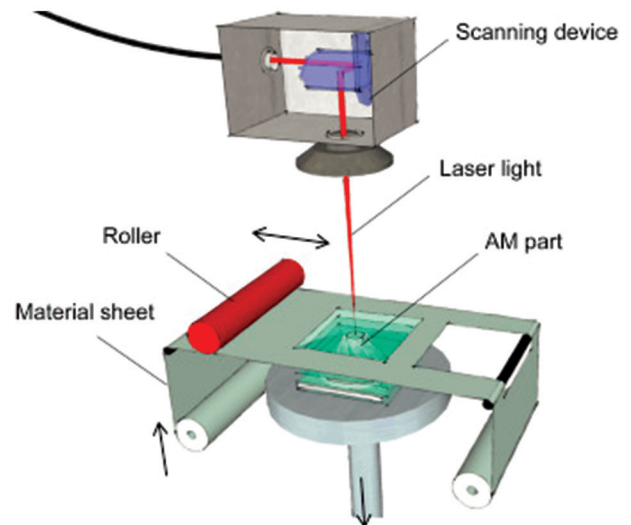

Figure 11. Schematic representation of laminated object manufacturing (Reprinted from Laser Additive Manufacturing, Hagedorn Y, *Laser additive manufacturing* of ceramic components: Materials, processes and mechanisms, pp. 163-180, Copyright (2017), with permission from Elsevier)[57].

production price, (iii) lower fragility or higher durability, (iv) a wide range of materials with versatile mechanical and chemical properties can be used in LOM, and (v) no post-processing is required. Unfortunately, the z-direction accuracy of LOM products is low.

2.7. Directed energy deposition (DED)

In DED methods, a focused energy source like laser and electron beam and plasma arc is utilized to melt the material, and the melted substance is deposited in the wire or in powder form through a nozzle. This method uses both features of material extrusion and power bed fusion AM processes. Unlike DED, the powder-bed fusion method melts the material during the deposition procedure[57]. In DED technique, the nozzle head can shift in multiple directions and around the fixed object according to the 3D CAD model. The high-energy beam is directed to the desired location to melt the material which immediately solidifies on the platform[58]. After the deposition of the initial layer, both nozzle and energy source shift upward to enable the deposition of the next layers on the previous ones, and this procedure is continued and repeated until the final 3D object is fabricated. The DED-based technique includes electron beam direct manufacturing, direct metal deposition (DMD), direct laser deposition, directed light fabrication, and laser engineered net shaping (LENS)[58]. These methods have the same processing steps but do not use the same energy source (type, power, and resolution), motion-control and powder delivery system, etc. **Figure 12** shows a schematic of the laser powder DED process.
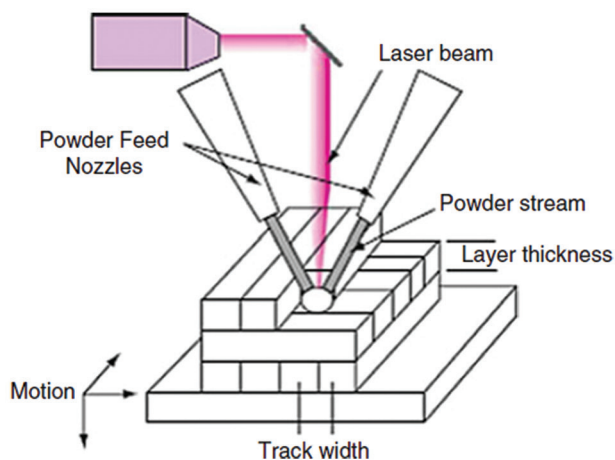
Figure 12. Schematic presentation of simple laser powder directed energy deposition technique (Reprinted from *Additive Manufacturing Technologies*, Directed energy deposition processes, 2015, pp. 245-168, Gibson I, Rosen D and Stucker B (original copyright notice as given in the publication in which the material was originally published) "With permission of Springer"[59].

3. AM in bioimplant applications

Until 2019, roughly 13% of annual 3DP revenues come directly from the medical industry. Medical experts can make use of AM technology to design patient-specific devices at an affordable cost. There are several reasons for the growing utilization of AM products in medicine: (i) Complex patient-specific implants and other specimens can be created by AM without any additional costs; (ii) 3D printed parts can be designed with high resolution (even nanometric ranges) to fit perfectly with a patient's anatomy; (iii) it is very easy to conduct sterilization during production and post-production stages on 3D printed samples; (iv) being a high-speed technology, AM can produce the implants at a rapid rate, thereby delivering therapies quickly; and (v) the flexible nature of AM technology significantly reduces the cost of custom medical devices. Considering these benefits, AM is utilized in many medical aspects, ranging from hearing aids, artificial limbs, surgical implants, bones, and blood cells to synthesized human organs[60]. Common applications of AM manufactured for biomedical applications are listed in **Table 1**[61].

3.1. Influencing parameters in biological response of 3D printed metals

(1) Pore size

In 3D printed metallic parts, two types of pores can be found; the first one is inter-particle pores and the second one is pre-designed pores. These pores can be arranged in an interconnected or non-interconnected manner that allows the formation of open or close porosity. Inter-particle pores are usually produced due to insufficient melting of metal powders, and afterward incomplete bonding but the fabrication of these inter-particle pores is totally undesirable. On the other hand, the pre-designed pores are in a regular arrangement and are particularly used for triggering osteoinduction, reduction of elastic modulus, and weight of implant[79-82]. The word "pore" in this review refers to the pre-designed version.

Pore size is among the crucial parameters which control the osteogenesis, migration of various cells, and supplement of nutrients and thus, the optimal pore size should be used in implant applications[83,84]. The favorable pore size for cell seeding should be in the range from 100 to 400 μm. It was reported that above this size range, cell seeding would become extremely difficult, the increased cell sizes are suitable for nutrients, waste, and blood transfer[85]. Cheng *et al*. produced porous Ti6Al4V constructs with different porosity and pore sizes through laser sintering and discussed the effects of 177-μm, 383-μm, and 653-μm pore sizes on biological behavior[86]. By increasing the pore size, the level of osteocalcin was increased and the alkaline phosphatase activity was reduced since it is more beneficial to maturation rather than proliferation. Another study confirmed that 500-μm pore sizes are better than 700- and 1000-μm ones from the osteogenic activity aspect since it seems that the optimum pore size range is about 300 – 600 μm[87].

It has been demonstrated that the heterogeneous pore size designs are very beneficial both from the mechanical property and biomedical reaction points of view[85,88]. The upgraded heterogenous gyroid structures with both coarse and fine pore sizes were produced by EBM through the control of cell wall spacing and the contribution of patterned extrude cuts onto the gyroid walls; hence, a dual bio-structural functionalization was achieved. Nutrient transportation can be improved by the smooth curvature of the gyroid walls. Moreover, the introduction of the micro-pores led to efficient bone cell seeding. This design has acceptable values of Young's modulus and compressive strength that are similar to those of the natural human bone[88]. In addition, Wang *et al*. produced a FEM-optimized heterogeneous porous lattice structure mimicking the human bone mechanical properties[85]. The produced structure includes a combination of micro-scaled pores for nutrients transfer and milli-scaled pores for cell seeding. The obtained results show the successful anisotropic design with mechanical properties similar to those of the human bone with the compressive strengths between 169 and 250 MPa, Young's modulus of 14 and 25 GPa, and densities of about 1.57 and 1.85 g/cm³.

(2) Porosity

Porosity simply shows the volume percentage of voids in a solid material which is measured in comparison

Table 1. Various AM technologies in medical applications and their advantages and disadvantages reproduced (Reprinted from 3D and 4D Printing of *Polymer Nanocomposite Materials,* Sinha SK, Additive manufacturing (AM) of medical devices and scaffolds for tissue engineering based on 3D and 4D printing, pp 119-160, Copyright (2020), with permission from Elsevier)[61]

Technique	Pros	Cons	References
Vat photopolymerization and Selective laser sintering	• High resolution • Enhanced mechanical property • Able to print high-density cells • Suitable for many photocurable polymers • The raw material base is a fluid • Complex structure formation through power bed • Biomaterial deposition in the solid or liquid phase • Able to use ceramic materials	• Shrinkage and heat effects • Material limitation • Require a UV source • Toxicity due to near UV blue light • Cell damage • Limitations in multicomponent cells • Thermal damage during the procedure	[62-68]
Stereolithography	• Great resolution and fast production • Independency of printing time to complexity • Nozzle-free technique	• Common for photopolymers • UV blue light is toxic to cells • Multicell printing is not possible	[69]
Powder fusion printing (PFP)	• High range of materials (metals, polymers, etc.) • Excellent mechanical strength • Complex geometries • Powder recycling	• Microfractures and voids • Crack generation • Hard to produce horizontal gradients • Need post processing • High power usage • Thermal distortion	[61,63]
Extrusion printing	• High simplicity • Excellent controlling • Capability to print both physical and compositional gradients • Capability to print cells and bioactive factors • Able to print polymers, metals, and ceramic parts	• Low speed • Only applicable for viscous liquids • Should control the material usage and other factors • Require binder/polymer removal at high temperature followed by sintering	[66,70,71]
Directed energy deposition	• The raw material platform is solid polymers • High resolution • No need to powder bed • Able to easily print multi-material structures along with compositional gradient	• Expensive procedure • Possibility of thermal damages • Poor part resolution and tolerances	[64-67,72]
Sheet lamination	• Speed, low cost, ease of material handling • Formation of layered laminate structure • Possibility to print hydroxyapatite, zirconia, various cells	• Just for layered laminates • Post-processing is needed • The strength and integrity of models are reliant on the adhesive used • May require post-processing • Limited material use	[64-67,73]
Indirect 3D printing	• Suitable for prototyping/preproduction • Applicable for various materials	• Low resolution • Time-consuming • Requirement for dedicated waxes for biocompatibility and molds for casting	[74]
Inkjet printing	• Applicable for wide range of biomaterials • Without any need to support structural complexities • High-speed • Coprinting the multiple solution compositions • It can simultaneously print bioactive composites • Materials with low viscosity can be printed	• Toxic nature • Compared to SLS, low mechanical strength • Expensive setup • Low applicable material range • Continuous procedures are not possible • Low cell density • Clogging of the head issues	[74,75]

(*Contd...*)

Table 1. (*Continued*)

Technique	Pros	Cons	References
Direct ink writing (DIW)	• Easy to use with hydrogels • Simple nature • Possibility to use multiple inks • Cost-effectiveness • Environmental friendliness	• It is not a good choice for complex parts and processes • Crucial to carefully control the thickening and thinning agents in bio-ink • Hard to attain the desired microstructure • Hard to extrude liquids	[76,77]
Fused deposition modeling (FDM)	• Lower toxicity compared to 3D printing with photopolymers • Cheap procedure	• Need to use additional support structure • Need to do post-processing • Low resolution	[78]
Bioplotting	• Possibility to print viable cells • Suitable for soft tissue	• Limited size ranges for nozzle • Need to use additional support structure	[74]
Laser-assisted bioprinting (LAB)	• Excellent precision printing • Single-cell patterns • It can use various bioactive materials • It can print different solutions at a time • Easy automation • High throughput	• Expensive • Scaffolds have limited heights	[74,77]

with materials without any pores. This parameter can be influenced by pore size, strut thickness, and pore shape. It is believed that higher porosities lead to better growth of osteon cells, increase the surface area which causes more cellular interactions, and provide proper interface-locking in laser-processed porous titanium[89]. Moreover, it has been shown that pore shape can affect osteogenic differentiation[90]. The improved osteogenic differentiation was observed on scaffolds with high porosities compared to low-density ones[91]. In fact, the porosity of human trabecular bone is within in the range of 70 – 90%, so this range seems to be suitable for a 3D printed implant. In a previous study by Cheng *et al.*, different porosities (70%, 37.9%, and 15%) were designed in EBM-produced Ti6Al4V samples, and the sample with the highest porosity has a higher potential for stimulating osteoblast differentiation than the other samples[92]. Other studies also confirmed this observation and asserted that implants with porosities similar to human bone's (70 – 90%) had the best bone ingrowth and greatly improved cell viability, but there would be some differences about the results of other biological responses toward porosity, like cell proliferation and differentiation[87,93].

(3) Interconnectivity of pores

The interconnectivity of pores determines whether the pores are connected or isolated. Formation of tissues in the interconnective structures can be progressively continued from the openings up to the central regions while dead ends due to isolated pore structures impede the growth of the cells and cause poor cellular interactions, such as differentiation, osteogenesis, and angiogenesis. Higher values of the influencing factors, such as detour indexes and pore throats, can sometimes lead to suppression of the proper bone ingrowth and tissue formation[94].

It is difficult to obtain the desired pore size and shape, porosity, and interconnection at the microscale level with traditional ways and evaluate their possible biological effects. However, it is rather simple to obtain well-designed and regular pore structures through AM technology. The CAD-based models can be utilized to predesign and produce any kind of porous structure using 3DP technologies. Two porous structures can be used: The honeycomb-like structure is a CAD-based structure with a diamond lattice, in which each atom is enveloped by four neighboring atoms[95,96], while the cubic structure is formed by scanning powder layers with the use of electron beams in constant intervals and parallel manner, and in every eighth layer, the scanning direction is rotated 90°[97].

(4) Lattice structure topologies

Many studies have focused on improving the lattice designs, especially on from the aspects of weight reduction and customizability, and various lattice structure topologies have therefore been proposed. In this regard, truss lattices with interconnecting struts in a 3D space are among the well-known class of lightweight parts. They have superior strength, stiffness, and energy

absorption capabilities[98]. The high-quality trusses with complex geometry and fine features can only be made by AM methods, specifically the SLM and EBM techniques. Some of the most popular truss lattices include simple cubic (SC), body-centered cubic (BCC), and face-centered cubic (FCC), as shown in **Figure 13**. These structures are made from the unification of vertical and inclined struts; for example, SC lattice includes vertical struts (and some tension in the horizontal struts) under compression; BCC consists of pure bended-inclined structure and FCC is a mixture of inclined struts with both bending and tension[98].

Structures can be categorized according to their geometrical features as shown in **Figure 13** the well-known truss lattices include: SC, BCC, and FCC. The structure with only some solid edges is called an open cell structure, whereas the structure with both solid edges and faces is known as a closed-cell structure. Foams have random connectivity of unit cells, and lattices have regular or periodic connectivity[99]. In this regard, other possible lattice structures and topologies were shown in **Figure 14** and include (a) Kagome, (b) octet truss, (c) MS1 lattice, (d) pillar textile, (e) square collinear/cubic, (f) re-entrant auxetic, (g) octahedron, (h) honeycomb, (i) square, (j) diamond, (k) triple periodic minimal surfaces (TPMS) P-type, (l) TPMS gyroid, (m) TPMS D-type, and (n) TPMS I-WP type[99]. It was found that topological features can affect the mechanical behavior of the material, and the octet truss design demonstrates superior mechanical properties, in addition to its ability to tolerate higher loads compared with other cellular structures. The main advantage of using cellular structure design is its ability in systematic and adroit utilization of material to reduce unnecessary consumption of material, energy, and time and manufacture lightweight parts with favorable mechanical strength[100]. Furthermore, cellular structures have a potential to show excellent thermal energy absorption and acoustic insulation properties[101]. From the aspects of geometry, porosity, and pores size, TPMS can be used as a topology suitable for manufacturing trabecular bone scaffolds[102].

3.2. Metallic scaffold parts in medicine

At present, metallic porous scaffolds are becoming one of the popular material choices in medical applications. One of the most important classes of materials in these applications is titanium (Ti) and its alloys due to its numerous mechanical advantages along with biocompatibility with living tissues[103-105]. Compared to stainless steel and other metallic systems, the medical-grade Ti-based alloys show enhanced performance, especially in bone tissue ingrowth capability since Ti has a 50% higher strength to weight ratio and less Young modulus in comparison to stainless steel[106-108]. Moreover, Ti-based materials are free of any toxic effects[109], and
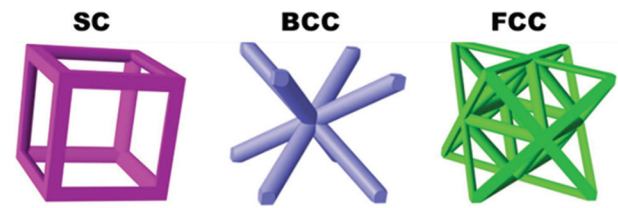

Figure 13. The most popular truss lattices: Simple cubic, body-centered cubic, and face-center-cubic (FCC) ((Reprinted from *Composites Part A: Applied Science and Manufacturing*, Volume 135, Li X, Tan YH, Wang P, *et al*, Metallic microlattice and epoxy interpenetrating phase composites: Experimental and simulation studies on superior mechanical properties and their mechanisms, Copyright (2020), with permission from Elsevier)[98].

they have acceptable mechanical properties (strength, elastic modulus, and hardness). In fact, the Young elastic modulus is of great importance in bone applications since a higher elastic modulus can lead to stress-shielding effect that could lead to implant failure; hence, the porous designs are preferred since they have a potential to control the stress-shielding effect[110]. Furthermore, Ti-based alloys exhibit excellent corrosion resistance in simulated body fluids[111,112]. Considering the above-mentioned superior features of Ti-based materials, 3DP of Ti is growing in importance for its application and bound to attract much attention. Recently, a successful case of 3DP of titanium was reported in a cancer patient; a 15-year-old boy received a Ti implant fabricated by the EOS Technology in a process that takes only about 6 weeks, starting from the CAD model designing model to the final implanting[61].

(1) Titanium-based porous structures

Recently, the AM manufactured porous structures attract much attention. Trabecular bone structure is one of the examples that can be designed by 3DP, and the obtained Ti porous structures can improve the bioactivity of implant, enhance cell adhesion, proliferation, and differentiation of osteoblasts[113]. Li *et al*. performed a systematic investigation about different aspects of 3D printed porous Ti-based materials that were produced by the EBM technique[114]. The highly porous and well-interconnected pore architecture shows good mechanical properties with enhancements in biological activity, osteoblast adhesion, cell morphology, proliferation, and alkaline phosphatase (ALP) activity. Moreover, to produce a Ti-based porous structure by the EBM technique, Zhang *et al*. designed a repeating array of titanium alloy unit-cells to mimic trabecular or cancellous bone structure[115]. Toward this end, various kinds of unit cells mimicking the trabecular bone structure with different pore sizes and porosity were produced. The result shows that the capacity of load-bearing is dependent on the porosity; a higher porosity value leads to a reduction of
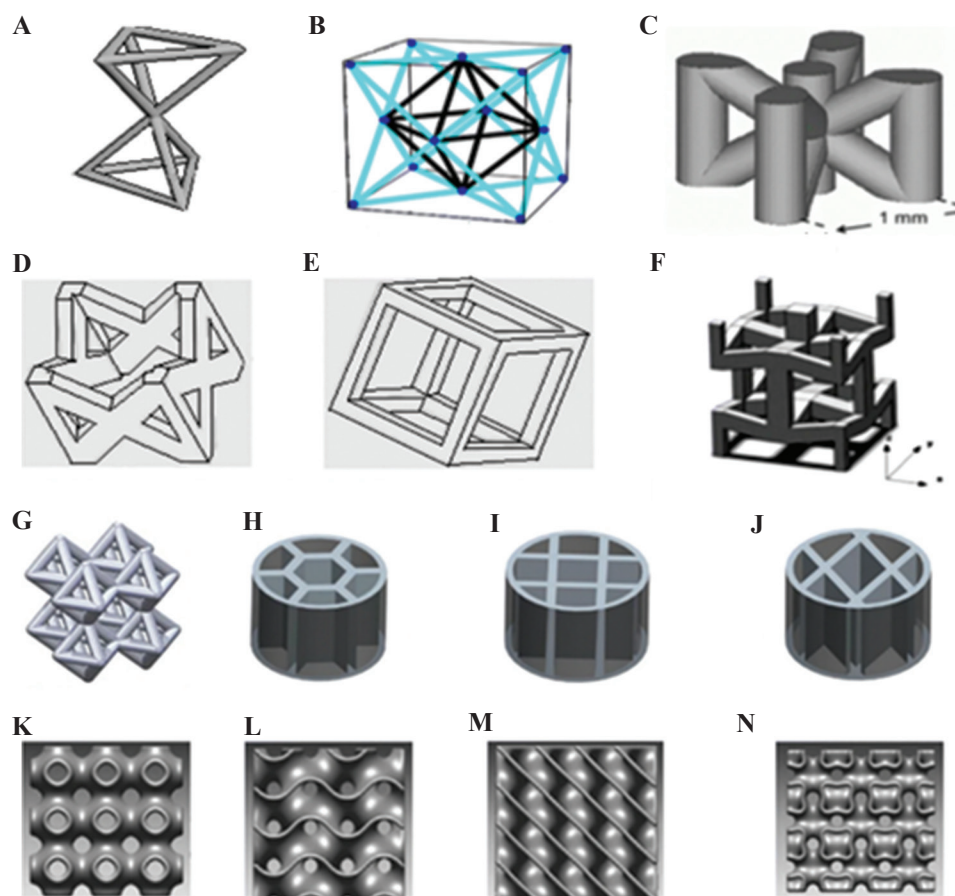
Figure 14. Various lattice structure topologies (*International Journal of Advanced Manufacturing Technology*, A state-of-the-art review on types, design, optimization, and additive manufacturing of cellular structures, Volume 104, 2019, pp. 3489–3510, Nazir A, Abate KM, Kumar A, *et al* (original copyright notice as given in the publication in which the material was originally published) "With permission of Springer")[99]. (A) Kagome, (B) octet truss, (C) MS1 lattice, (D) pillar textile, (E) square collinear/cubic, (F) re-entrant auxetic, (G) octahedron, (H) honeycomb, (I) square, (J) diamond, (K) triple periodic minimal surfaces (TPMS) P-type, (L) TPMS gyroid, (M) TPMS D-type, and (N) TPMS I-WP type.

stiffness and load capacity; compared to dense Ti material, the 3D printed porous structure manifested a 96% decrease in elastic modulus and strength values.

AM manufactured porous titanium interbody cages are very useful in spine treatment, and they have desirable levels of biocompatibility that is beneficial for better bone ingrowth and fixation. A comparative *in vivo* study that utilized 3D printed titanium porous implants produced by Stryker on several mature sheep found that bone ingrowth on porous titanium alloy was superior to both PEEK and plasma spray-coated implants and the histomorphometric results showed better osteoblastic deposition on these implants[116]. Furthermore, peri-implant osteogenesis and increased stability were observed in 3D printed titanium samples. The titanium porous materials can be further improved in different strategies. For instance, Song *et al.* capitalized upon the varying macro architectures and surface topological morphology on SLM produced porous titanium for modulation[117]. This dual modulation

was initially carried out together with the utilization of a wide range of compressive strengths and subsequently by alkali treatment, heat treatment, and hydroxyapatite coating formation through electrochemical deposition. The *in vitro* results indicated good cytocompatibility, improved osteon cell adhesion, and proliferation, while *in vivo* experiments indicated superior tissue-materials interfaces in dual modulated samples. **Figure 15** shows the fabrication method of dual modulation on 3D printed titanium material.

Coating with biologically beneficial substances is one of the methods for improving AM manufactured porous materials. Bose *et al.*[118] manufactured titanium porous structures with about 25% volume porosity through LENS method, produced TiO_2 nanotubes on the structure surface and a coating functionalized by Sr^{2+} and Si^{4+} ions, doped bioactive calcium phosphate (CaP) ceramic in simulated body fluid and implanted the samples in the rat model. These doped CaP-coated 3D printed Ti implants
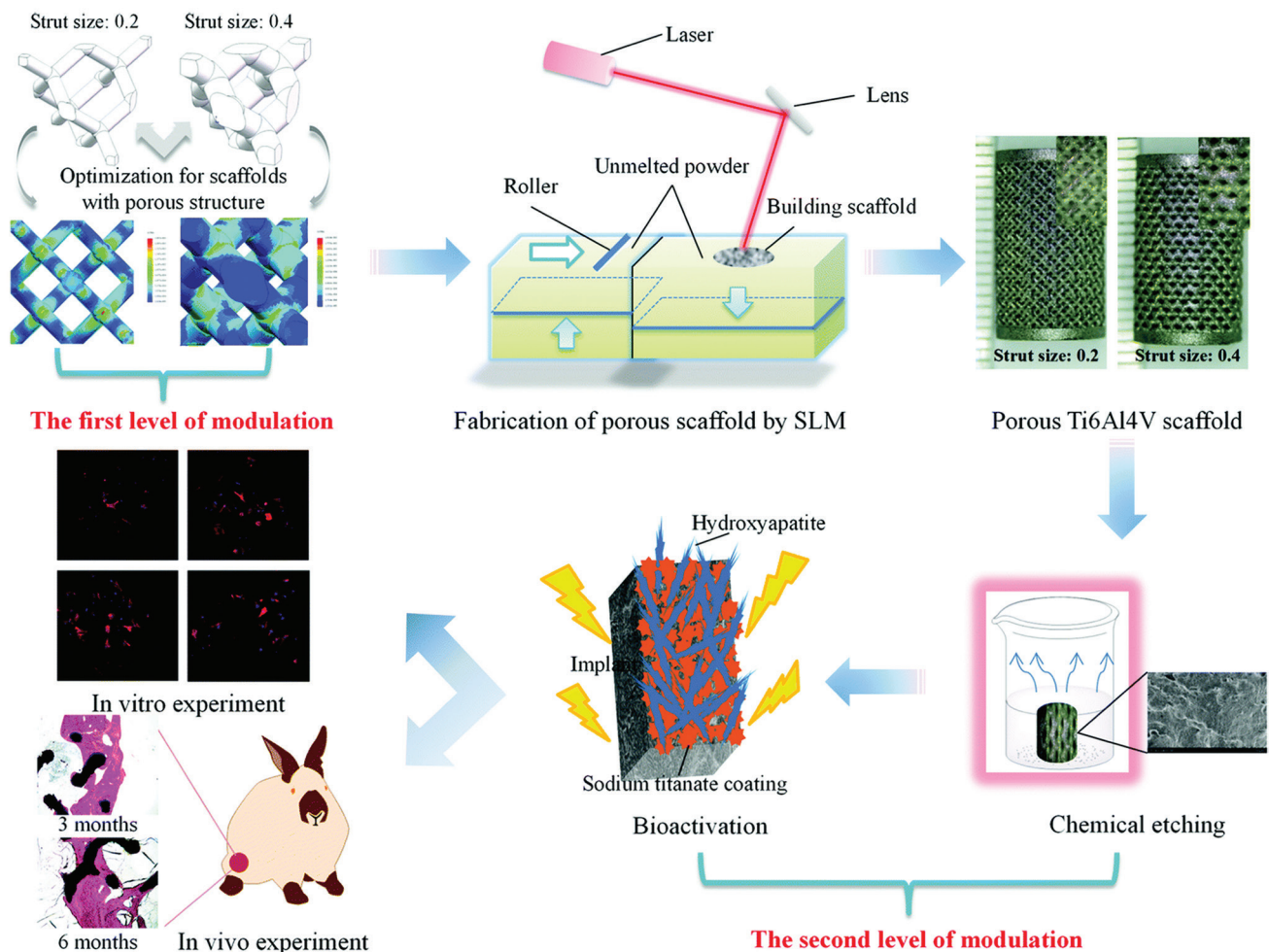
Figure 15. Schematic presentation of the dual modulation procedure (Adapted from Ref [117] with permission from The Royal Society of Chemistry).

resulted in early bone tissue integration and proper tissue ingrowth. Furthermore, a good bonding in the interfacial regions between the bone tissue and the implant surface was observed. Moreover, it enhanced new bone formation and accelerated mineralization were seen in the periphery of the implant material. Overall, porous materials have better biological performance than the dense type. Furthermore, CaP plays a crucial role in early bone tissue integration with the implant. **Figure 16** shows a brief explanation about doping and coating procedure.

Among the titanium-based biomaterials, Ti6Al4V is known for its improved mechanical properties relative to the pure Ti. Unfortunately, the toxic effects of Al and V restrict its application in clinical settings. Nevertheless, since the release of Al and V is in low amounts, Ti6Al4V can still be used in medical devices and implants. Many studies have been performed to examine the design parameters, such as porosity and pore size, in relation to this subject. **Table 2** presents a brief review of these studies.

The production of 3D printed titanium porous structure is progressing toward the commercial stage; for instance, U.S. Food and Drug Administration (FDA) has approved the 3D printed titanium implants, which are known as Emerging Implant Technologies (EIT) Cellular Titanium® (**Figure 17**) produced by a German medical device manufacturer, for spinal applications. This new product was designed based on the ideal pore shape and size, with the goal to achieve improved cell proliferation and bone ingrowth conditions. In fact, the EIT cervical cage's anatomical architecture can potentially overcome the surgical and biomechanical issues related to the cervical multi-level fusion by modifying the vertebral endplate contact and sagittal balance restoration[126]. Another example approved by FDA is the MATRIXX® stand-alone cervical system for patients suffering from degenerative disc treatment will be assisted by it. Furthermore, a number of companies that utilize direct metal printing technology, such as IMR, nuVasive, and Stryker, are working on production AM manufactured titanium implants[127].
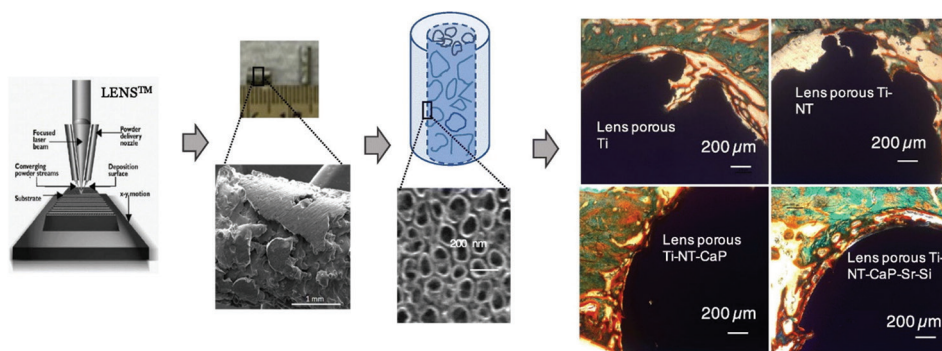
Figure 16. Schematic presentation of Sr^{+2} and Si^{+4} doped CaP coating on 3D printed porous titanium with nanoscale surface modification (Reprinted from *Materials & Design*, Volume 151, Bose S, Banerjee D, Shivaram A, *et al*, Calcium phosphate coated 3D printed porous titanium with nanoscale surface modification for orthopedic and dental applications, pp 102-112, Copyright (2018), with permission from Elsevier)[119].
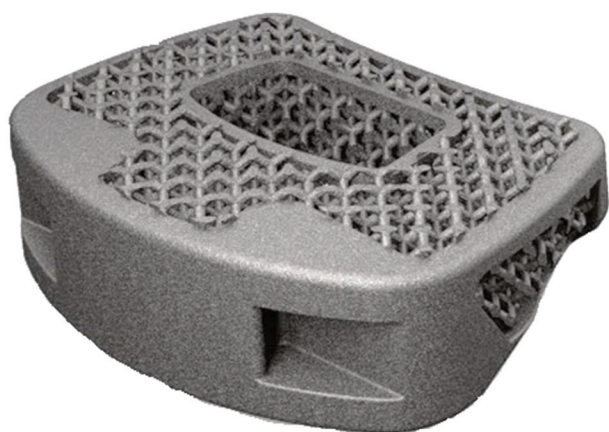

Figure 17. Emerging Implant Technologies (EIT) cervical cage or the EIT Cellular Titanium® approved by the U.S. Food and Drug Administration[126].

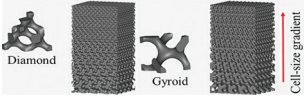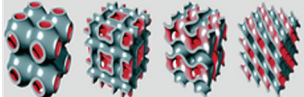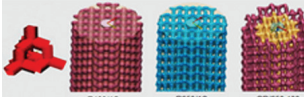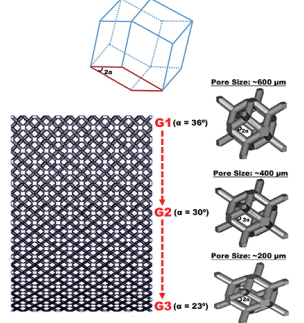### (2) 3D printed cobalt chromium (CoCr) alloys

In orthopedic surgery, CoCr-based alloys are of significant importance and utilized extensively in high loaded areas. Nonetheless, the stress shielding effect and bone resorption are the major concerns when it comes to applications due to the high stiffness level of CoCr alloys[128]. Smart design and structural modifications can help overcome these issues; one of the best options to reduce the stiffness mismatch in metal-alloy implants' interface and the periphery natural bone tissue is designing the porous structures. In this regard, additively manufactured CoCr alloys have attracted much attention. Shah *et al*. produced a 3D printed CoCr alloy specimen with interconnected open-pore architecture and macro-geometry with EBM technology[129]. The produced samples were implanted in adult sheep femora and the outcomes after 26 weeks revealed that the density of osteocyte was higher in the CoCr sample compared to that in Ti6Al4V, but the total bone-implant contact of

Ti6Al4V was higher. Furthermore, the CoCr alloy does not significantly change the mineralized interfacial tissue composition compared to Ti6Al4V alloy. Overall, the results indicated the possibility of bone in growth in the interconnected porous structure of CoCr samples. In a different study, Limmahakhun *et al*. studied the micro-pore structure, biological response, and mechanical properties of CoCr alloy scaffolds that were produced by SLM and reported that the SLM techniques are capable of fabricating the CoCr cellular structures with graded beam thickness and the unit cells with pillar-octahedral shape and human bones share the similar mechanical properties and morphology[130].

(3) 3D printed tantalum
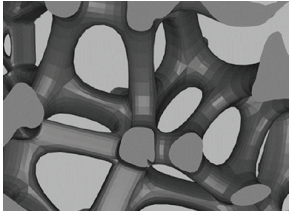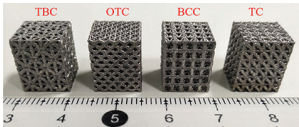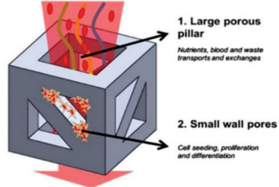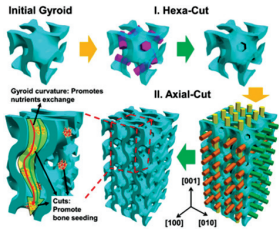
Tantalum is an inert material both in *in vivo* and *in vitro* condition and has low solubility and very low toxicity in its pure and oxide forms. Tantalum behavior in hard tissues is similar to titanium with osteointegration properties. This material has been clinically utilized since 1940 and its applications in implantation and diagnosis are growing[131]. The characteristics of tantalum, which are similar to that of cancellous bone, enable its applications in orthopedic surgeries in the spine and hip, knee arthroplasty, and as bone graft substitutes. Levine *et al*.[132] studied the porous tantalum structure which was produced through carbon vapor deposition/infiltration onto vitreous carbon scaffolding. This open-cell design with continuous dodecahedrons unit cells indicated enhanced volumetric porosity (70 – 80%), low Young's modulus (~3 MPa), and improved frictional properties. Furthermore, it has good biocompatibility and can produce a self-passivating surface oxide layer which is beneficial for biological applications. Therefore, tantalum is an appropriate option for biomedical applications, and 3DP of tantalum would be a good way to further improve its features. In 2017, a Chinese research group performed

Table 2. Brief information about the characteristics and outcomes of 3D printed Ti-based porous scaffolds

AM method	Characteristics	Results	References
SLM	 Diamond lattice pore structure, porosity 66.1 – 79.5%, pore size 0.65 mm, strut diameter 0.2 – 0.4 mm	Dimensional accuracy is dependent on printing parameters, such as laser power, scanning speed, and power layer thickness. The 10% porosity reduction results in a 100-MPa increase in compression strength. New inward bone tissue growth was observed in both cancellous and compact bone within 0.4 mm strut diameter and 66.1% porosity	[4]
SLM	 Interconnecting channels with various diameters (500, 700, and 900 μm)	Well-defined pore distribution with proper interconnectivity, the small pores are helpful for cell adhesion, the large pores improve cell proliferation. Pores with about 600-μm size are beneficial for bone ingrowth, maturation, and bone-implant fixation stability	[119]
SLM	 Three gradient patterns (cell size, density, heterostructure), gyroid and diamond unit cells with triply periodic minimal surfaces (TPMS)	The TPMS method is suitable for obtaining functional graded structures that mimic natural bone. Gyroid and diamond unit cells possess a suitable strength (152.6 MPa and 145.7 MPa) and comparable elastic modulus (3.8 GPa) with compact bone. The pore size gradient does not lead to considerable density alterations	[120]
SLM	 TPMS porous structures, from left to right: primitive, I-WP, gyroid, and diamond	TMPS structures well resembled the topological properties of trabecular bone, high fatigue resistance, and endurance limit as high as 60% of their yield stress. It has comparable morphology and permeability values with trabecular bone. Excellent mechanical properties such as low elastic modulus and high yield strength	[121]
SLM	 Dense center and graded periphery structure, porosity in the range of 50 – 80%	Other favorable properties are high compressive strength, improvement of bone integration, enhanced cell growth, maximum calcium deposition in 400 um pore size, and better osteointegration. Spider web structures show higher Young's modulus values. Web structures (70% porosity) and diamond unit structures (porosity 50%) share almost similar mechanical properties	[122]
EBM	 Dodecahedron unit cells with various pore sizes (600, 400, and 200 μm). Porosity 65%, with 500 μm strut sizes	Porous structure minimizes the stress-shielding effect. Other beneficial effects are increased osteoblasts function, cell adhesion, proliferation, proteins' function, and calcium deposition. Smaller pore sizes have better biological performance than larger ones	[123]

Table 2. (*Continued*)

AM method	Characteristics	Results	References
SLM	 Trabecular like scaffolds based on the Voronoi Tessellation principle with a porosity range of 48.83 – 74.28% and varying irregularities (0.05 – 0.5)	This scaffold has the elastic modulus in the range of 1.93-5.24GPa and an ultimate strength ranging within 44.9- 237.5 MPa, enhanced osteoblasts adhesion and migration, improved cell proliferation, and early osteoblast differentiation	[124]
SLM	 Exterior with octet truss cell (75% porosity and pore size of 1042 μm) and internal structure with tetrahedron cell (80% porosity and pore size of 700 μm)	SLM has high accuracy in printing CAD modeled scaffolds associated with cell proliferation of about 140% which is superior to that of about 90% in other uniform structures. Hence, these porous functional graded structures are a better option for bone implant applications.	[125]
EBM	 Heterogeneous porous micro lattices with the coarse central porous pillar and fine pores within walls. Nutrients exchange through micro-scaled pores and milli-scaled pores are responsible for cell seeding, porosities up to ~ 60%	The mechanical properties of microlattices are in the range of the same parameters of human cortical bone. In addition, their compressive strengths and Young's modulus are in the range of 169.5 – 250.9 MPa and 14.7 – 25.3 GPa, respectively. The existence of edges to close up the lattice boundaries enhances the mechanical properties. The anisotropic design could improve structural efficiency in a specific loading direction	[85]
EBM	 Upgraded gyroid lattices, gyroid wall spacings in millimeter range and additional micrometer-scaled pores on the walls	The wide wall spacing facilitates nutrients transports into the implant, and the micro-pores are responsible for seeding the bone cells. The stress-shield effect is inhibited by maintaining the Young's modulus values between 8 and 15 GPa. The compressive strength was in the range of 150 – 250 MPa. The mechanical properties fall within the natural range of the human bone	[88]

SLM, selective laser melting; EBM, electron beam melting.

a total knee replacement using the 3D printed tantalum on an 84-year-old man who was able to do some basic movements only a day after the surgery[133]. Despite the challenges in the 3DP of tantalum due to the high melting temperature (~3000°C), the produced samples are still praiseworthy for being very compact and having fewer defects.

(4) Shape memory alloys (SMA)

The shape memory effect is a unique phenomenon in which the deformed material has the ability to recover to its original shape and size when heated in a special characteristic temperature range or as a response to mechanical stresses by a reversible martensitic transformation. This impressive feature bequeaths the

SMA many applications, especially in medical and spine surgeries[134-136]. Moreover, the SMAs also have other stimulating uses in actuators, sensors, the aerospace industry, and even fashion products[137].

One of the most imperative classes of SMAs in medical applications is NiTi alloys. In addition to its very interesting shape memory effect, NiTi has good ductility, outstanding corrosion and wear resistance, and terrific biocompatibility[137]. This section focuses only on NiTi or nitinol since they are the most utilized SMAs. Manufacturing parameters can largely influence the functionality of SMAs, texture, microstructure, surface quality, precipitates, and several defects[138,139]; hence, the production process needs to be precisely controlled. LAM methods, including LSM, are highly utilized in the production of 3D printed SMAs since these methods ensure proper homogeneity, especially in complex and dense structures. Furthermore, these methods are applied in the production of various-shaped SMAs because they can produce graded porous structures accurately. Usually, SLM method and laser metal deposition (LMD) are commonly used in the production of 3D printed SMAs (**Figure 18**). Both methods utilize metal powders and the sample is produced by cross-sectional slicing of the CAD model and layer by layer deposition. In SLM, special regions in a metal powder bed are melted and solidified, while in LMD, several nozzles are used to feed successive layers of powders onto the building substrate on which the powder is melted by laser exposure. Several key parameters that influence the final quality of 3D printed part should be considered while using either one of both methods. These parameters include material condition (powder size, morphology, and composition), machine parameters (laser type, atmosphere), processing variables (laser power, track spacing, scanning rate and pattern, powder layer thickness, and beam spot diameter), and power feed rate in LDM method.

Achieving the highest material density is of high importance in 3DP. In SLM, increasing the density of laser-energy leads to enhancement of component density up to the maximum value. After this peak, density reduction is possible, especially in materials which are vulnerable to oxidation and evaporation materials. This issue is very crucial in NiTi alloys since slight changes in composition can alter the shape memory effect of the material. Powder re-melting can potentially homogenize and eliminate the local compositional variations and enhance the overall SMA effect. Reducing the SLM scan speed and increasing SLM energy density can increment the transformation temperature and leads to a better temperature SMA temperature range[140,141].

NiTi SMA has excellent corrosion and wears resistance along with desirable biocompatibility which is attributed to the formation of the titanium oxide layer on its surface. This layer has a protective nature and even prevents the possible toxic and allergic effects of Ni release; therefore, the thicker TiO_2 layers are preferred[142,143]. Laser irradiation can influence the TiO_2 formation and thickness which affects its biocompatibility. For instance, Nd-YAG laser irradiation has very beneficial effect on corrosion improvement and prevention of Ni ion release. This Nd-YAG laser irradiation can produce a thick oxide layer inhibiting the corrosion while retaining other properties[144]. Moreover, to enhance the biological response of the material and mesenchymal stem cells, the metal AM fiber lasers (optical fibers that doped with rare-earth elements) can be a good option since they are associated with desirable surface parameters, such as increased roughness and wettability, and improved surface chemistry[145].

A review of research literature shows that 3D printed NiTi alloys are potential candidates for implantation as they act as a good host for living cells and tissues. Habijan *et al*.[146] showed that the surface of SLM-produced porous NiTi scaffolds was entirely covered with live cells with a very insignificant number of dead cells after 8 days of cell culture. Other similar studies on SLM-produced porous
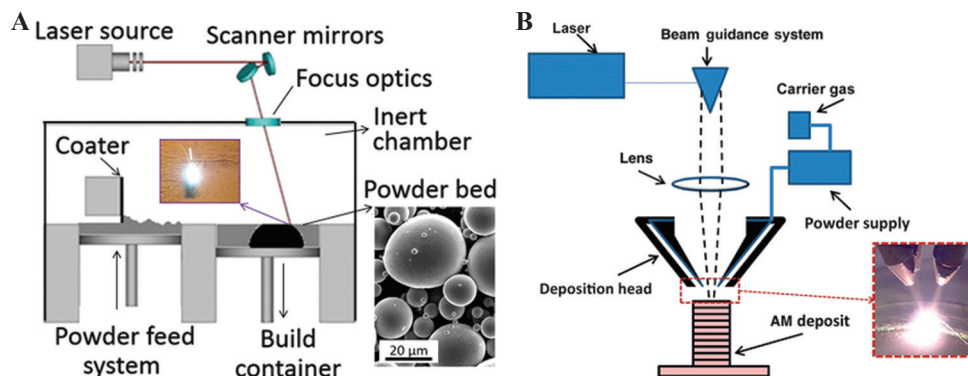

Figure 18. Schematic presentation of (A) selective laser melting method with a scanning electron microscope image of powder and (B) laser metal deposition process with a metal deposition condition (Reproduced from Ref. [137] with permission from Cambridge University Press, https://doi.org/10.1557/mrs.2016.209, Copyright 2016 Materials Research Society 2016).
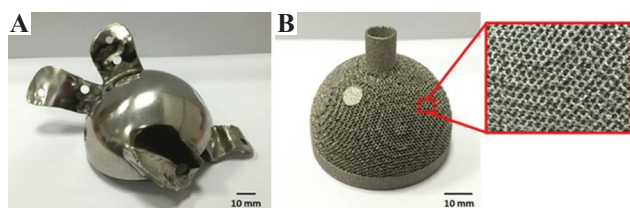
Figure 19. The 3D printed NiTi samples. (A) Selective laser melting-produced hip joint after polishing. (B) Electron beam melting-produced acetabular cup and the magnified view of the porous lattice structure (Reproduced from Ref [152] with permission from Wiley Periodicals, Inc., https://doi.org/10.1002/jor.23075, Copyright 2015 Orthopaedic Research Society

NiTi scaffolds through osteogenic cell culture confirms the good mechanical properties and successful activity of osteogenic stem cells in a salty medium or even under-controlled compression stresses[147-149]. Furthermore, it was found that Ni ion release was below the cytotoxic level in both dense and AM produced porous NiTi scaffolds and reduced laser-beam diameter can decline the Ni ion release in SLM-produced NiTi scaffolds[146,150]. **Figure 19** shows examples of 3D printed NiTi components that have medical applications.

4. Conclusions

The 3D printed implants have attracted much attention in recent years since they are amenable to rapid production, custom-built design, and precise control over the dimension and porosity. In this regard, the present review focuses on the history of various AM methods that are utilized in the production of metallic implants. Different technologies and effective parameters are discussed. Furthermore, the porous 3D printed metallic scaffolds that are lighter in weight, osteoconductive, can prevent stress-shield effect, and form interconnected structures to facilitate the nutrients transformation and cell growth is a subject of discussion in this review. Moreover, the 3DP of various imperative metallic systems for titanium, Ti6Al4V alloy, CoCr alloy, tantalum, and SMA are introduced. Considering the growing attention and utilization of AM manufactured products in medicine, it is necessary to develop more sophisticated technologies that have more precise control over the effective parameters in biological environments. These new technologies need to fulfill some key requirements, such as fast production, higher resolution of products, economical and environmentally friendly methods, less defective procedures, proper custom-built designs, biocompatibility, resistance to corrosion, wear, and compressive loads, inhibition of stress-shielding effects, proper surface conditions (roughness, wettability), and antibacterial designs. Recently, the emergence of smart and novel methods, including 4D printing, seems to represent a revolutionary

step in AM technology. This review briefly summarizes the current knowledge in 3DP of implants with a special emphasis on the technologies and procedures which are instrumental in the conception and development of de novo technologies.

Acknowledgments

Conflicts of interest

The authors declare no conflicts of interest.

Data availability

All data generated or analyzed during this study are included in this published article.

References

1. Ni J, Ling H, Zhang S, *et al*., 2019, Three-dimensional Printing of Metals for Biomedical Applications. *Mater Today Bio*, 3:100024.
   https://doi.org/10.1016/j.mtbio.2019.100024.

2. Attaran M, 2017, The Rise of 3-D Printing: The Advantages of Additive Manufacturing Over Traditional Manufacturing. *Bus Horiz*, 60:677–88.
   https://doi.org/10.1016/j.bushor.2017.05.011.

3. Skylar-Scott MA, Uzel SG, Nam LL, *et al*., 2019, Biomanufacturing of Organ-specific Tissues with High Cellular Density and Embedded Vascular Channels. *Sci Adv*, 5:eaaw2459.
   https://doi.org/10.1126/sciadv.aaw2459.

4. Zhang B, Pei X, Zhou C, *et al*., 2018, The Biomimetic Design and 3D Printing of Customized Mechanical Properties Porous Ti6Al4V Scaffold for Load-bearing Bone Reconstruction. *Mater Des*, 152:30–9.
   https://doi.org/10.1016/j.matdes.2018.04.065.

5. Söhling N, Neijhoft J, Nienhaus V, *et al*., 2020, 3D-Printing of Hierarchically Designed and Osteoconductive Bone Tissue Engineering Scaffolds. *Materials* (*Basel*), 13:1836.
   https://doi.org/10.3390/ma13081836.

6. Pei X, Ma L, Zhang B, *et al*., 2017, Creating Hierarchical Porosity Hydroxyapatite Scaffolds with Osteoinduction by Three-dimensional Printing and Microwave Sintering. *Biofabrication*, 9:45008.
   https://doi.org/10.1088/1758-5090/aa90ed.

7. Stepniak K, Ursani A, Paul N, *et al*., 2020, Novel 3D Printing

Technology for CT Phantom Coronary Arteries with High Geometrical Accuracy for Biomedical Imaging Applications. *Bioprinting*, 18:e00074.

https://doi.org/10.1016/j.bprint.2020.e00074.

8. Jardini AL, Larosa MA, Filho RM, *et al.*, 2014, Cranial Reconstruction: 3D Biomodel and Custom-built Implant Created Using Additive Manufacturing. *J Craniomaxillofac Surg*, 42:1877–84.

https://doi.org/10.1016/j.jcms.2014.07.006.

9. Mobbs RJ, Coughlan M, Thompson R, *et al.*, 2017, The Utility of 3D Printing for Surgical Planning and Patient-specific Implant Design for Complex Spinal Pathologies: Case Report. *J Neurosurg Spine*, 26:513–8.

https://doi.org/10.3171/2016.9.SPINE16371.

10. Kodama H, 1981, A Scheme for Three-Dimensional Display by Automatic Fabrication of Three-Dimensional Model. *IEICE Trans Electron* (*Japanese Ed*), 64:237–41.

11. Hull CW, Spence ST, Albert DJ, *et al.*, 1988, Methods and Apparatus for Production of Three-dimensional Objects by Stereolithography, Patents No. 5059359.

12. Noor N, Shapira A, Edri R, *et al.*, 2019, 3D Printing of Personalized Thick and Perfusable Cardiac Patches and Hearts. *Adv Sci*, 2019:1900344.

https://doi.org/10.1002/advs.201900344.

13. Ahmad AN, Gopinath P, Vinogradov A, 2019, 3D Printing in Medicine. In: 3D Printing Technology, Nanomedicine. Elsevier, Amsterdam, Netherlands, pp. 1–22.

https://doi.org/10.1016/B978-0-12-815890-6.00001-3.

14. Gorsse S, Hutchinson C, Gouné M, *et al.*, 2017, Additive Manufacturing of Metals: A Brief Review of the Characteristic Microstructures and Properties of Steels, Ti-6Al-4V and High-entropy Alloys. *Sci Technol Adv Mater*, 18:584–610.

https://doi.org/10.1080/14686996.2017.1361305.

15. Boularaoui S, Al Hussein G, Khan KA, *et al.*, 2020, An Overview of Extrusion-based Bioprinting with a Focus on Induced Shear Stress and its Effect on Cell Viability. *Bioprinting*, 20:e00093.

https://doi.org/10.1016/j.bprint.2020.e00093.

16. Gibson I, Rosen D, Stucker B, 2015, Vat Photopolymerization Processes. In: Addition Manufacturing Technologies. Springer, New York, pp. 63–106.

https://doi.org/10.1007/978-1-4939-2113-3_4.

17. Appuhamillage GA, Chartrain N, Meenakshisundaram V, *et al.*, 2019, 110th Anniversary : Vat Photopolymerization-Based Additive Manufacturing: Current Trends and Future Directions in Materials Design. *Ind Eng Chem Res*, 58:15109–18.

https://doi.org/10.1021/acs.iecr.9b02679.

18. Shirazi SF, Gharehkhani S, Mehrali M, *et al.*, 2015, A Review on Powder-based Additive Manufacturing for Tissue Engineering: Selective Laser Sintering and Inkjet 3D Printing. *Sci Technol Adv Mater*, 16:033502.

https://doi.org/10.1088/1468-6996/16/3/033502.

19. Sun S, Brandt M, Easton M, 2017, 2-Powder Bed Fusion Processes: An Overview. In: Brandt MB, editor. Woodhead Publishing Series in Electronic and Optical Materials. Woodhead Publishing, Sawston, United Kingdom, pp. 55–77.

https://doi.org/https://doi.org/10.1016/B978-0-08-100433-3.00002-6.

20. Sing SL, Huang S, Yeong WY, 2020, Effect of Solution Heat Treatment on Microstructure and Mechanical Properties of Laser Powder Bed Fusion Produced Cobalt-28chromium-6molybdenum. *Mater Sci Eng A*, 769:138511.

https://doi.org/10.1016/j.msea.2019.138511.

21. Galati M, Iuliano L, 2018, A Literature Review of Powder-based Electron Beam Melting Focusing on Numerical Simulations. *Addit Manuf*, 19:1–20.

https://doi.org/https://doi.org/10.1016/j.addma.2017.11.001.

22. Yu W, Sing SL, Chua CK, *et al.*, 2019, Influence of Re-melting on Surface Roughness and Porosity of AlSi10Mg Parts Fabricated by Selective Laser Melting. *J Alloys Compd*, 792:574–81.

https://doi.org/10.1016/j.jallcom.2019.04.017.

23. Li X, Tan YH, Willy HJ, *et al.*, 2019, Heterogeneously Tempered Martensitic High Strength Steel by Selective Laser Melting and its Micro-lattice: Processing, Microstructure, Superior Performance and Mechanisms. *Mater Des*, 178:107881.

https://doi.org/10.1016/j.matdes.2019.107881.

24. Kuo CN, Chua CK, Peng PC, *et al.*, 2020, Microstructure Evolution and Mechanical Property Response via 3D Printing Parameter Development of Al-Sc alloy. *Virtual Phys Prototyp*, 15:120–9.

https://doi.org/10.1080/17452759.2019.1698967.

25. Yap CY, Chua CK, Dong ZL, *et al.*, 2015, Review of Selective Laser Melting: Materials and Applications. *Appl Phys Rev*, 2:041101.

https://doi.org/10.1063/1.4935926.

26. Sing SL, Wiria FE, Yeong WY, 2018, Selective Laser Melting of Titanium Alloy with 50 wt% Tantalum: Effect of Laser Process Parameters on Part Quality. *Int J Refract Met Hard Mater*, 77:120–7.

https://doi.org/10.1016/j.ijrmhm.2018.08.006.

27. Wang P, Nai ML, Tan X, *et al.*, 2016, Recent Progress

of Additive Manufactured Ti-6Al-4V by Electron Beam Melting. In: Solid Free from fabrication. 2016 Proceeding 27th Annual International Solid Freeform Fabrication Symposium Additive Manufacturing. Conference, pp. 691–704.

28. Nandwana P, Lee Y, 2020, Influence of Scan Strategy on Porosity and Microstructure of Ti-6Al-4V Fabricated by Electron Beam Powder Bed Fusion. *Mater Today Commun*, 24:100962.
https://doi.org/10.1016/j.mtcomm.2020.100962.

29. Tan JH, Sing SL, Yeong WY, 2020, Microstructure Modelling for Metallic Additive Manufacturing: A Review. *Virtual Phys Prototyp*, 15:87–105.
https://doi.org/10.1080/17452759.2019.1677345.

30. Wang P, Tan X, Nai ML, *et al*., 2016, Spatial and Geometrical-based Characterization of Microstructure and Microhardness for an Electron Beam Melted Ti-6Al-4V Component. *Mater Des*, 95:287–95.
https://doi.org/10.1016/j.matdes.2016.01.093.

31. Galarraga H, Lados DA, Dehoff RR, *et al*., 2016, Effects of the Microstructure and Porosity on Properties of Ti-6Al-4V ELI Alloy Fabricated by Electron Beam Melting (EBM). *Addit Manuf*, 10:47–57.
https://doi.org/10.1016/j.addma.2016.02.003.

32. Wang P, Nai ML, Sin WJ, *et al*., 2018, Realizing a Full Volume Component by *In-Situ* Welding during Electron Beam Melting Process. *Addit Manuf*, 22:375–80.
https://doi.org/10.1016/j.addma.2018.05.022.

33. Wang P, Goh MH, Li Q, *et al*., 2020, Effect of Defects and Specimen Size with Rectangular Cross-section on the Tensile Properties of Additively Manufactured Components. *Virtual Phys Prototyp*, 15:251–64.
https://doi.org/10.1080/17452759.2020.1733430.

34. Pan Wang JW, Sin WJ, Nai ML, 2017, Effects of Processing Parameters on Surface Roughness of Additive Manufactured Ti-6Al-4V via Electron Beam Melting. *Materials* (*Basel*), 10:1121.
https://doi.org/10.3390/ma10101121.

35. Zhang LC, Chen LY, Wang L, 2020, Surface Modification of Titanium and Titanium Alloys: Technologies, Developments, and Future Interests. *Adv Eng Mater*, 22: 1901258.
https://doi.org/10.1002/adem.201901258.

36. Singh R, Singh S, Hashmi MS, 2016, Implant Materials and Their Processing Technologies. In: The Reference Module in Materials Science and Materials Engineering. Elsevier, Amsterdam, Netherlands.
https://doi.org/10.1016/B978-0-12-803581-8.04156-4.

37. Körner C, 2016, Additive Manufacturing of Metallic Components by Selective Electron Beam Melting a Review. *Int Mater Rev*, 61:361–77.
https://doi.org/10.1080/09506608.2016.1176289.

38. Chia HN, Wu BM, 2015, Recent Advances in 3D Printing of Biomaterials. *J Biol Eng*, 9:4.
https://doi.org/10.1186/s13036-015-0001-4.

39. Waheed S, Cabot JM, Macdonald NP, *et al*., 2016, 3D Printed Microfluidic Devices: Enablers and Barriers. *Lab Chip*, 16:1993–2013.
https://doi.org/10.1039/C6LC00284F.

40. Zhang Y, Jarosinski W, Jung YG, *et al*., 2018, Additive Manufacturing Processes and Equipment. In: Additive Manufacturing. Elsevier, Amsterdam, Netherlands, pp. 39–51.
https://doi.org/10.1016/B978-0-12-812155-9.00002-5.

41. Upcraft S, Fletcher R, 2003, The Rapid Prototyping Technologies. *Assem Autom*, 23:318–30.
https://doi.org/10.1108/01445150310698634.

42. Hwang HH, Zhu W, Victorine G, *et al*., 2018, 3D-Printing of Functional Biomedical Microdevices via Light and Extrusion-Based Approaches. *Small Methods*, 2:1700277.
https://doi.org/10.1002/smtd.201700277.

43. Pilipović A, RaosP, Šercer M, 2009, Experimental Analysis of Properties of Materials for Rapid Prototyping. *Int J Adv Manuf Technol*, 40:105–15.
https://doi.org/10.1007/s00170-007-1310-7.

44. Bhattacharjee N, Urrios A, Kang S, *et al*., 2016, The Upcoming 3D-Printing Revolution in Microfluidics. *Lab Chip*, 16:1720–42.
https://doi.org/10.1039/C6LC00163G.

45. Hamid Q, Snyder J, Wang C, *et al*., 2011, Fabrication of Three-dimensional Scaffolds Using Precision Extrusion Deposition with an Assisted Cooling Device. *Biofabrication*, 3:034109.
https://doi.org/10.1088/1758-5082/3/3/034109.

46. Vaezi M, Zhong G, Kalami H, *et al*., 2018, Extrusion-based 3D Printing Technologies for 3D Scaffold Engineering. In: Functional 3D Tissue Engineering Scaffolds: Materials, Technologies, and Applications. Elsevier, Amsterdam, Netherlands, pp. 235–54.
https://doi.org/10.1016/B978-0-08-100979-6.00010-0.

47. Greulich M, Greul M, Pintat T, 1995, Fast, Functional Prototypes via Multiphase Jet Solidification. *Rapid Prototyp J*, 1:20-5.
https://doi.org/10.1108/13552549510146649.

48. Carneiro OS, Silva AF, Gomes R, 2015, Fused Deposition Modeling with Polypropylene. *Mater Des*, 83:768–76.
https://doi.org/10.1016/j.matdes.2015.06.053.

49. Sun L, Parker ST, Syoji D, *et al*., 2012, Direct-Write Assembly of 3D Silk/Hydroxyapatite Scaffolds for Bone Co-Cultures. *Adv Healthc Mater*, 1:729–35.
https://doi.org/10.1002/adhm.201200057.

50. Rane K, Strano M, 2019, A Comprehensive Review of Extrusion-based Additive Manufacturing Processes for Rapid Production of Metallic and Ceramic Parts. *Adv Manuf*, 7:155–73.
https://doi.org/10.1007/s40436-019-00253-6.

51. Highley CB, 2019, 3D Bioprinting Technologies. In: 3D Bioprinting Medicine. Springer International Publishing, Cham, Switzerland, pp. C1–2.
https://doi.org/10.1007/978-3-030-23906-0_8.

52. El Aita I, Breitkreutz J, Quodbach J, 2019, On-demand Manufacturing of Immediate Release Levetiracetam Tablets Using Pressure-assisted Microsyringe Printing. *Eur J Pharm Biopharm*, 134:29–36.
https://doi.org/10.1016/j.ejpb.2018.11.008.

53. Vaezi M, Seitz H, Yang S, 2013, A Review on 3D Micro-additive Manufacturing Technologies. *Int J Adv Manuf Technol*, 67:1957–7.
https://doi.org/10.1007/s00170-013-4962-5.

54. Mekonnen BG, Bright G, Walker A, 2016, A Study on State of the Art Technology of Laminated Object Manufacturing (LOM). Springer, Berlin, Germany, pp. 207–16.
https://doi.org/10.1007/978-81-322-2740-3_21.

55. Dermeik B, Travitzky N, 2020, Laminated Object Manufacturing of Ceramic-Based Materials. *Adv Eng Mater*, 2020:2000256.
https://doi.org/10.1002/adem.202000256.

56. Hagedorn Y, 2017, Laser Additive Manufacturing of Ceramic Components. In: Laser Additive Manufacturing. Elsevier, Amsterdam, Netherlands, pp. 163–80.
https://doi.org/10.1016/B978-0-08-100433-3.00006-3.

57. Horn TJ, Harrysson OL, 2012, Overview of Current Additive Manufacturing Technologies and Selected Applications. *Sci Prog*, 95:255–82.
https://doi.org/10.3184/003685012X13420984463047.

58. Gibson I, Rosen DW, Stucker B, 2009, Additive Manufacturing Technologies: Rapid Prototyping to Direct Digital Manufacturing. Springer US, Berlin, Germany.
https://doi.org/10.1007/978-1-4419-1120-9.

59. Gibson I, Rosen D, Stucker B, 2015, Directed Energy Deposition Processes. In: Addition Manufacturing Technologies. Springer, New York, pp. 245–68.
https://doi.org/10.1007/978-1-4939-2113-3_10.

60. Ventola CL, 2014, Medical Applications for 3D Printing: Current and Projected Uses. *P T*, 39:704–11.

61. Sinha SK, 2020, Additive Manufacturing (AM) of Medical Devices and Scaffolds for Tissue Engineering Based on 3D and 4D Printing. In: 3D 4D Printing of Polymer Nanocomposite Materials. Elsevier, Amsterdam, Netherlands, pp. 119–60.
https://doi.org/10.1016/B978-0-12-816805-9.00005-3.

62. Wang D, Wang Y, Wu S, *et al*., 2017, Customized a Ti6Al4V Bone Plate for Complex Pelvic Fracture by Selective Laser Melting. *Materials* (*Basel*), 10:35.
https://doi.org/10.3390/ma10010035.

63. Turnbull G, Clarke J, Picard F, *et al*., 2018, 3D Bioactive Composite Scaffolds for Bone Tissue Engineering. *Bioact Mater*, 3:278–314.
https://doi.org/10.1016/j.bioactmat.2017.10.001.

64. Roopavath UK, Kalaskar DM, 2017, Introduction to 3D Printing in Medicine. In: 3D Printing in Medicine. Elsevier, Amsterdam, Netherlands, pp. 1–20.
https://doi.org/10.1016/B978-0-08-100717-4.00001-6.

65. Wang X, Ao Q, Tian X, *et al*., 2016, 3D Bioprinting Technologies for Hard Tissue and Organ Engineering. *Materials* (*Basel*). 9:802.
https://doi.org/10.3390/ma9100802.

66. Derakhshanfar S, Mbeleck R, Xu K, *et al*., 2018, 3D Bioprinting for Biomedical Devices and Tissue Engineering: A Review of Recent Trends and Advances. *Bioact Mater*, 3:144–56.
https://doi.org/10.1016/j.bioactmat.2017.11.008.

67. Nagarajan N, Dupret-Bories A, Karabulut E, *et al*., 2018, Enabling Personalized Implant and Controllable Biosystem Development through 3D Printing. *Biotechnol Adv*, 36, 521–33.
https://doi.org/10.1016/j.biotechadv.2018.02.004.

68. Bandyopadhyay A, Mitra I, Bose A, 2020, 3D Printing for Bone Regeneration. *Curr Osteoporos Rep*, 18:505–14.
https://doi.org/10.1007/s11914-020-00606-2.

69. Bittner SM, Guo JL, Melchiorri A, *et al*., 2018, Three-dimensional Printing of Multilayered Tissue Engineering Scaffolds. *Mater Today*, 21:861–74.
https://doi.org/10.1016/j.mattod.2018.02.006.

70. Chang J, He J, Mao M, *et al*., 2018, Advanced Material Strategies for Next-Generation Additive Manufacturing. *Materials* (*Basel*), 11:166.
https://doi.org/10.3390/ma11010166.

71. Peng F, Vogt BD, Cakmak M, 2018, Complex Flow and Temperature History during Melt Extrusion in Material Extrusion Additive Manufacturing. *Addit Manuf*, 22:197–206.
https://doi.org/10.1016/j.addma.2018.05.015.

72. Bandyopadhyay A, Traxel KD, 2018, Invited Review Article:

Metal-additive Manufacturing Modeling Strategies for Application-optimized Designs. *Addit Manuf*, 22:758–74. https://doi.org/10.1016/j.addma.2018.06.024.

73. Thakar CM, Deshmukh SP, Mulla TA, 2020, A Review on Selective Deposition Lamination 3D Printing Technique. *Int J Adv Sci Res Eng Trends*, 4:7–11.

74. Do AV, Smith R, Acri TM, Geary SM, *et al*., 2018, 3D Printing Technologies for 3D Scaffold Engineering. In: Functional 3D Tissue Engineering Scaffolds: Materials, Technologies, and Applications. Elsevier, Amsterdam, Netherlands, pp. 203–34. https://doi.org/10.1016/B978-0-08-100979-6.00009-4.

75. Devillard R, Pagès E, Correa MM, *et al*., 2014, Cell Patterning by Laser-Assisted Bioprinting. *Methods Cell Biol*, 119:159-74. https://doi.org/10.1016/B978-0-12-416742-1.00009-3.

76. Akbari S, Zhang YF, Wang D, *et al*., 2018, 4D Printing and its Biomedical Applications. In: 3D 4D Printing in Biomedical Applications. Wiley-VCH Verlag GmbH and Co., KGaA, Weinheim, Germany, pp. 343–72. https://doi.org/10.1002/9783527813704.ch14.

77. Hao L, Tang D, Sun T, *et al*., 2020, Direct Ink Writing of Mineral Materials: A review. *Int J Precis Eng Manuf Technol*, 1:266. https://doi.org/10.1007/s40684-020-00222-6.

78. An J, Teoh JE, Suntornnond R, *et al*., 2015, Design and 3D Printing of Scaffolds and Tissues. *Engineering*, 1:261–8. https://doi.org/10.15302/J-ENG-2015061.

79. Krishna BV, Xue W, Bose S, *et al*., 2008, Engineered Porous Metals for Implants. *JOM*, 60: 45–8. https://doi.org/10.1007/s11837-008-0059-2.

80. Yang J, Gu D, Lin K, *et al*., 2020, Laser 3D Printed Bio-inspired Impact Resistant Structure: Failure Mechanism under Compressive Loading. *Virtual Phys Prototyp*, 15:75–86. https://doi.org/10.1080/17452759.2019.1677124.

81. du Plessis A, Razavi SM, Berto F, 2020, The Effects of Microporosity in Struts of Gyroid Lattice Structures Produced by Laser Powder Bed Fusion. *Mater Des*, 194:108899. https://doi.org/10.1016/j.matdes.2020.108899.

82. Meng L, Zhao J, Lan X, *et al*., 2020, Multi-objective Optimisation of Bio-inspired Lightweight Sandwich Structures Based on Selective Laser Melting. *Virtual Phys Prototyp*, 15:106–19. https://doi.org/10.1080/17452759.2019.1692673.

83. Matena J, Petersen S, Gieseke M, *et al*., 2015, SLM Produced Porous Titanium Implant Improvements for Enhanced Vascularization and Osteoblast Seeding. *Int J Mol Sci*, 16:7478–92. https://doi.org/10.3390/ijms16047478.

84. Van Cleynenbreugel T, Schrooten J, Van Oosterwyck H, *et al*., 2006, Micro-CT-based Screening of Biomechanical and Structural Properties of Bone Tissue Engineering Scaffolds. *Med Biol Eng Comput*, 44:517–25. https://doi.org/10.1007/s11517-006-0071-z.

85. Wang P, Li X, Jiang Y, *et al*., 2020, Electron Beam Melted Heterogeneously Porous Microlattices for Metallic Bone Applications: Design and Investigations of Boundary and Edge Effects. *Addit Manuf*, 36:101566. https://doi.org/10.1016/j.addma.2020.101566.

86. Cheng A, Humayun A, Cohen DJ, *et al*., 2014, Additively Manufactured 3D Porous Ti-6Al-4V Constructs Mimic Trabecular Bone Structure and Regulate Osteoblast Proliferation, Differentiation and Local Factor Production in a Porosity and Surface Roughness Dependent Manner. *Biofabrication*, 6:045007. https://doi.org/10.1088/1758-5082/6/4/045007.

87. Markhoff J, Wieding J, Weissmann V, *et al*., 2015, Influence of Different Three-Dimensional Open Porous Titanium Scaffold Designs on Human Osteoblasts Behavior in Static and Dynamic Cell Investigations. *Materials* (*Basel*), 8:5490–507. https://doi.org/10.3390/ma8085259.

88. Wang P, Li X, Luo S, *et al*., 2021, Additively Manufactured Heterogeneously Porous Metallic Bone with Biostructural Functions and Bone-like Mechanical Properties. *J Mater Sci Technol*, 62:173–9. https://doi.org/10.1016/j.jmst.2020.05.056.

89. Xue W, Krishna BV, Bandyopadhyay A, *et al*., 2007, Processing and Biocompatibility Evaluation of Laser Processed Porous Titanium. *Acta Biomater*, 3:1007–18. https://doi.org/10.1016/j.actbio.2007.05.009.

90. Balla VK, Bodhak S, Bose S, *et al*., 2010, Porous Tantalum Structures for Bone Implants: Fabrication, Mechanical and *In Vitro* Biological Properties. *Acta Biomater*, 6:3349–59. https://doi.org/10.1016/j.actbio.2010.01.046.

91. Jeon H, Lee H, Kim G, 2014, A Surface-Modified Poly(ε-caprolactone) Scaffold Comprising Variable Nanosized Surface-Roughness Using a Plasma Treatment. *Tissue Eng Part C Methods*, 20:951–63. https://doi.org/10.1089/ten.tec.2013.0701.

92. Lv J, Jia Z, Li J, *et al*., 2015, Electron Beam Melting Fabrication of Porous Ti6Al4V Scaffolds: Cytocompatibility and Osteogenesis. *Adv Eng Mater*, 17:1391–8. https://doi.org/10.1002/adem.201400508.

93. Biemond JE, Aquarius R, Verdonschot N, *et al*., 2011, Frictional and Bone Ingrowth Properties of Engineered Surface Topographies Produced by Electron Beam

Technology. *Arch Orthop Trauma Surg*, 131:711–8. https://doi.org/10.1007/s00402-010-1218-9.

94. Otsuki B, Takemoto M, Fujibayashi S, *et al*., 2006, Pore Throat Size and Connectivity Determine Bone and Tissue Ingrowth into Porous Implants: Three-dimensional Micro-CT Based Structural Analyses of Porous Bioactive Titanium Implants. *Biomaterials*, 27:5892–900. https://doi.org/10.1016/j.biomaterials.2006.08.013.

95. Rumpler M, Woesz A, Dunlop JW, *et al*., 2008, The Effect of Geometry on Three-dimensional Tissue Growth. *J R Soc Interface*, 5:1173–80. https://doi.org/10.1098/rsif.2008.0064.

96. Marin E, Fusi S, Pressacco M, *et al*., 2010, Characterization of Cellular Solids in Ti6Al4V for Orthopaedic Implant Applications: Trabecular Titanium. *J Mech Behav Biomed Mater*, 3:373–81. https://doi.org/10.1016/j.jmbbm.2010.02.001.

97. Parthasarathy J, Starly B, Raman S, *et al*., 2010, Mechanical Evaluation of Porous Titanium (Ti6Al4V) Structures with Electron Beam Melting (EBM). *J Mech Behav Biomed Mater*, 3:249–59. https://doi.org/10.1016/j.jmbbm.2009.10.006.

98. Li X, Tan YH, Wang P, *et al*., 2020, Metallic Microlattice and Epoxy Interpenetrating Phase Composites: Experimental and Simulation Studies on Superior Mechanical Properties and their Mechanisms. *Compos Part A Appl Sci Manuf*, 135:105934. https://doi.org/10.1016/j.compositesa.2020.105934.

99. Nazir A, Abate KM, Kumar A, *et al*., 2019, A State-of-the-art Review on Types, Design, Optimization, and Additive Manufacturing of Cellular Structures. *Int J Adv Manuf Technol*, 104:3489–510. https://doi.org/10.1007/s00170-019-04085-3.

100. Parthasarathy J, Starly B, Raman S, 2011, A Design for the Additive Manufacture of Functionally Graded Porous Structures with Tailored Mechanical Properties for Biomedical Applications. *J Manuf Process*, 13:160–70. https://doi.org/10.1016/j.jmapro.2011.01.004.

101. Gibson LJ, Ashby MF, 1999, Cellular Solids: Structure and Properties. Cambridge University Press, Cambridge, United Kingdom. https://doi.org/10.1017/CBO9781139878326.

102. Fantini M, Curto M, De Crescenzio F, 2017, TPMS for Interactive Modelling of Trabecular Scaffolds for Bone Tissue Engineering BT Advances on Mechanics, Design Engineering and Manufacturing : Proceedings of the International Joint Conference on Mechanics, Design Engineering and Advanced Manufactur. In: Eynard B, Nigrelli V, Oliveri SM, Peris-Fajarnes G, Rizzuti S, editors. Springer International Publishing, Cham, Switzerland, pp. 425–35. https://doi.org/10.1007/978-3-319-45781-9_43.

103. Attarilar S, Salehi MT, Al-Fadhalah KJ, *et al*., 2019, Functionally Graded Titanium Implants: Characteristic Enhancement Induced by Combined Severe Plastic Deformation. *PLoS One*, 14:1–18. https://doi.org/10.1371/journal.pone.0221491.

104. Roach P, Eglin D, Rohde K, *et al*., 2007, Modern Biomaterials: A Review Bulk Properties and Implications of Surface Modifications. *J Mater Sci Mater Med*, 18:1263–77. https://doi.org/10.1007/s10856-006-0064-3.

105. Triyono J, Alfiansyah R, Sukanto H, *et al*., 2020, Fabrication and Characterization of Porous Bone Scaffold of Bovine Hydroxyapatite-glycerin by 3D Printing Technology. *Bioprinting*, 18:e00078. https://doi.org/10.1016/j.bprint.2020.e00078.

106. Wang Q, Zhou P, Liu S, *et al*., 2020, Multi-Scale Surface Treatments of Titanium Implants for Rapid Osseointegration: A Review. *Nanomaterials*, 10:1244. https://doi.org/10.3390/nano10061244.

107. Wang P, Todai M, Nakano T, 2019, Beta titanium Single Crystal with Bone-like Elastic Modulus and Large Crystallographic Elastic Anisotropy. *J Alloys Compd*, 782:667–71. https://doi.org/10.1016/j.jallcom.2018.12.236.

108. Wang P, Wu L, Feng Y, *et al*., 2017, Microstructure and Mechanical Properties of a Newly Developed Low Young's Modulus Ti-15Zr-5Cr-2Al Biomedical Alloy. *Mater Sci Eng C*, 72:536–42. https://doi.org/10.1016/j.msec.2016.11.101.

109. Attarilar S, Yang J, Ebrahimi M, *et al*., 2020, The Toxicity Phenomenon and the Related Occurrence in Metal and Metal Oxide Nanoparticles: A Brief Review From the Biomedical Perspective. *Front Bioeng Biotechnol*, 8:822. https://doi.org/10.3389/fbioe.2020.00822.

110. Niinomi M, Nakai M, 2011, Titanium-Based Biomaterials for Preventing Stress Shielding between Implant Devices and Bone. *Int J Biomater*, 2011:836587. https://doi.org/10.1155/2011/836587.

111. Gode C, Attarilar S, Eghbali B, *et al*., 2015, Electrochemical Behavior of Equal Channel Angular Pressed Titanium for Biomedical Application. AIP Conference Proceedings, United States. https://doi.org/10.1063/1.4914232.

112. Attarilar S, Djavanroodi F, Irfan OM, *et al*., 2020, Strain Uniformity Footprint on Mechanical Performance and

Erosion-corrosion Behavior of Equal Channel Angular Pressed Pure Titanium. *Results Phys*, 17:103141. https://doi.org/10.1016/j.rinp.2020.103141.

113. Taniguchi N, Fujibayashi S, Takemoto M, *et al*., 2016, Effect of Pore Size on Bone Ingrowth into Porous Titanium Implants Fabricated by Additive Manufacturing: An *In Vivo* Experiment. *Mater Sci Eng C*, 59:690–701. https://doi.org/10.1016/j.msec.2015.10.069.

114. Li X, Ma XY, Feng YF, *et al*., 2015, A Novel Composite Scaffold Consisted of Porous Titanium and Chitosan Sponge for Load-bearing Applications: Fabrication, Characterization and Cellular Activity. *Compos Sci Technol*, 117:78–84. https://doi.org/10.1016/j.compscitech.2015.05.019.

115. Zhang C, Zhang L, Liu L, *et al*., 2020, Mechanical Behavior of a Titanium Alloy Scaffold Mimicking Trabecular Structure. *J Orthop Surg Res*, 15:40. https://doi.org/10.1186/s13018-019-1489-y.

116. McGilvray KC, Easley J, Seim HB, *et al*., 2018, Bony Ingrowth Potential of 3D-Printed Porous Titanium Alloy: A Direct Comparison of Interbody Cage Materials in an *In Vivo* Ovine Lumbar Fusion Model. *Spine J*, 18:1250–60. https://doi.org/10.1016/j.spinee.2018.02.018.

117. Song P, Hu C, Pei X, *et al*., 2019, Dual Modulation of Crystallinity and Macro-/Microstructures of 3D Printed Porous Titanium Implants to Enhance Stability and Osseointegration. *J Mater Chem B*, 7:2865–77. https://doi.org/10.1039/C9TB00093C.

118. Bose S, Banerjee D, Shivaram A, *et al*., 2018, Calcium Phosphate Coated 3D Printed Porous Titanium with Nanoscale Surface Modification for Orthopedic and Dental Applications. *Mater Des*, 2018:S0264127518303198. https://doi.org/10.1016/j.matdes.2018.04.049.

119. Ran Q, Yang W, Hu Y, *et al*., 2018, Osteogenesis of 3D Printed Porous Ti6Al4V Implants with Different Pore Sizes. *J Mech Behav Biomed Mater*, 84:1–11. https://doi.org/10.1016/j.jmbbm.2018.04.010.

120. Liu F, Mao Z, Zhang P, *et al*., 2018, Functionally Graded Porous Scaffolds in Multiple Patterns: New Design Method, Physical and Mechanical Properties. *Mater Des*, 160:849–60. https://doi.org/10.1016/j.matdes.2018.09.053.

121. Bobbert FS, Lietaert K, Eftekhari AA, *et al*., 2017, Additively Manufactured Metallic Porous Biomaterials Based on Minimal Surfaces: A Unique Combination of Topological, Mechanical, and Mass Transport Properties. *Acta Biomater*, 53:572–84. https://doi.org/10.1016/j.actbio.2017.02.024.

122. Wally ZJ, Haque AM, Feteira A, *et al*., 2019, Selective Laser Melting Processed Ti6Al4V Lattices with Graded Porosities for Dental Applications. *J Mech Behav Biomed Mater*, 90:20–9. https://doi.org/10.1016/j.jmbbm.2018.08.047.

123. Nune KC, Kumar A, Misra RD, *et al*., 2017, Functional Response of Osteoblasts in Functionally Gradient Titanium Alloy Mesh Arrays Processed by 3D Additive Manufacturing. *Colloids Surf B Biointerfaces*, 150:78–88. https://doi.org/10.1016/j.colsurfb.2016.09.050.

124. Liang H, Yang Y, Xie D, *et al*., 2019, Trabecular-like Ti-6Al-4V Scaffolds for Orthopedic: Fabrication by Selective Laser Melting and *In Vitro* Biocompatibility. *J Mater Sci Technol*, 35:1284–97. https://doi.org/10.1016/j.jmst.2019.01.012.

125. Wang S, Liu L, Li K, *et al*., 2019, Pore Functionally Graded Ti6Al4V Scaffolds for Bone Tissue Engineering Application. *Mater Des*, 168:107643. https://doi.org/10.1016/j.matdes.2019.107643.

126. Yosra K, 2018, EIT Emerging Implant Technology Granted FDA Multilevel Approval for their 3D Printed Cervical Cage, SPINEMarketGroup. Available from: https://3dadept.com/eit-emerging-implant-technology-granted-fda-multilevel-approval-for-their-3d-printed-cervical-cage/. [Last accessed on 2020 Nov 30].

127. Martial Y, 2019, Nexxt Spine creates 3D Printed Porous Titanium Interbodies Using GE Additive's Mlab Printer. Available from: https://3dadept.com/nexxt-spine-creates-3d-printed-porous-titanium-interbodies-using-ge-additives-mlab-printer/. [Last accessed on 2020 Nov 30].

128. Semba JA, Mieloch AA, Rybka JD, 2020, Introduction to the State-of-the-art 3D Bioprinting Methods, Design, and Applications in Orthopedics. *Bioprinting*, 18:e00070. https://doi.org/10.1016/j.bprint.2019.e00070.

129. Shah FA, Omar O, Suska F, *et al*., 2016, Long-term Osseointegration of 3D Printed CoCr Constructs with an Interconnected Open-pore Architecture Prepared by Electron Beam Melting. *Acta Biomater*, 36:296–309. https://doi.org/10.1016/j.actbio.2016.03.033.

130. Limmahakhun S, Oloyede A, Sitthiseripratip K, *et al*., 2017, Stiffness and Strength Tailoring of Cobalt Chromium Graded Cellular Structures for Stress-shielding Reduction. *Mater Des*, 114:633–41. https://doi.org/10.1016/j.matdes.2016.11.090.

131. Black J, 1994, Biologic Performance of Tantalum. *Clin Mater*, 16:167–73. https://doi.org/10.1016/0267-6605(94)90113-9.

132. Levine BR, Sporer S, Poggie RA, *et al*., 2006, Experimental and Clinical Performance of Porous Tantalum in Orthopedic

Surgery. *Biomaterials*, 27:4671–81.
https://doi.org/10.1016/j.biomaterials.2006.04.041.

133. Saunders S, 2017, Chinese Hospital Uses 3D Printed Tantalum Implant in Successful Knee Replacement Surgery. Available from: https://3dprint.com/195286/3d-printed-tantalum-knee-implant/. [Last accessed on 2020 Nov 30].

134. Wever D, Elstrodt J, Veldhuizen A, *et al*., 2002, Scoliosis Correction with Shape-memory Metal: Results of an Experimental Study. *Eur Spine J*, 11:100–6.
https://doi.org/10.1007/s005860100347.

135. Wang Y, Zheng G, Zhang X, *et al*., 2011, Temporary Use of Shape Memory Spinal Rod in the Treatment of Scoliosis. *Eur Spine J*, 20:118–22.
https://doi.org/10.1007/s00586-010-1514-7.

136. Márquez JM, Pérez-Grueso, Fernández-Baíllo N, *et al*., 2012, Gradual Scoliosis Correction Over Time with Shape-memory Metal: A Preliminary Report of an Experimental Study. *Scoliosis*, 7:20.
https://doi.org/10.1186/1748-7161-7-20.

137. Dadbakhsh S, Speirs M, Van Humbeeck J, *et al*., 2016, Laser Additive Manufacturing of Bulk and Porous Shape-memory NiTi Alloys: From Processes to Potential Biomedical Applications. *MRS Bull*, 41:765–74.
https://doi.org/10.1557/mrs.2016.209.

138. Liu Y, Xie ZL, Van Humbeec J, *et al*., 1999, Effect of Texture Orientation on the Martensite Deformation of NiTi Shape Memory Alloy Sheet. *Acta Mater*, 47:645–60.

139. Motemani Y, Nili-Ahmadabadi M, Tan MJ, *et al*., 2009, Effect of Cooling Rate on the Phase Transformation Behavior and Mechanical Properties of Ni-rich NiTi Shape Memory Alloy. *J Alloys Compd*, 469:164–8.
https://doi.org/10.1016/j.jallcom.2008.01.153.

140. Dadbakhsh S, Speirs M, Kruth JP, *et al*., 2014, Effect of SLM Parameters on Transformation Temperatures of Shape Memory Nickel Titanium Parts. *Adv Eng Mater*, 16:1140–6.
https://doi.org/10.1002/adem.201300558.

141. Bormann T, Schumacher R, Müller B, *et al*., 2012. Tailoring Selective Laser Melting Process Parameters for NiTi Implants. *J Mater Eng Perform*, 21:2519–24.
https://doi.org/10.1007/s11665-012-0318-9.

142. Figueira N, Silva TM, Carmezim MJ, *et al*., 2009, Corrosion Behaviour of NiTi Alloy. *Electrochim Acta*, 54:921–6.

https://doi.org/10.1016/j.electacta.2008.08.001.

143. Muhonen V, Heikkinen R, Danilov A, *et al*., 2007, The Effect of Oxide Thickness on Osteoblast Attachment and Survival on NiTi Alloy. *J Mater Sci Mater Med*, 18:959–67.
https://doi.org/10.1007/s10856-006-0082-1.

144. Cui ZD, Man HC, Yang XJ, 2005, The Corrosion and Nickel Release Behavior of Laser Surface-melted NiTi Shape Memory Alloy in Hanks' Solution. *Surf Coatings Technol*, 192:347–53.
https://doi.org/10.1016/j.surfcoat.2004.06.033.

145. Chan CW, Hussain I, Waugh DG, *et al*., 2014, Effect of Laser Treatment on the Attachment and Viability of Mesenchymal Stem Cell Responses on Shape Memory NiTi Alloy. *Mater Sci Eng C*, 42:254–63.
https://doi.org/10.1016/j.msec.2014.05.022.

146. Habijan T, Haberland C, Meier H, *et al*., 2013, The Biocompatibility of Dense and Porous Nickel-Titanium Produced by Selective Laser Melting. *Mater Sci Eng C*, 33:419–26.
https://doi.org/10.1016/j.msec.2012.09.008.

147. Strauß S, Dudziak S, Hagemann R, *et al*., 2012, Induction of Osteogenic Differentiation of Adipose Derived Stem Cells by Microstructured Nitinol Actuator-Mediated Mechanical Stress. *PLoS One*, 7:e51264.
https://doi.org/10.1371/journal.pone.0051264.

148. Liu S, Liu J, Wang L, *et al*., 2020, Superelastic Behavior of *In-Situ* Eutectic-Reaction Manufactured High Strength 3D Porous NiTi-Nb Scaffold. *Sci Mater*, 181:121–6.
https://doi.org/10.1016/j.scriptamat.2020.02.025.

149. Hafeez N, Liu J, Wang L, *et al*., 2020, Superelastic Response of Low-modulus Porous Beta-type Ti-35Nb-2Ta-3Zr Alloy Fabricated by Laser Powder Bed Fusion. *Addit Manuf*, 34:101264.
https://doi.org/10.1016/j.addma.2020.101264.

150. Putters JL, Sukul K, de Zeeuw GR, *et al*., 1992, Comparative Cell Culture Effects of Shape Memory Metal (Nitinol), Nickel and Titanium: A Biocompatibility Estimation. *Eur Surg Res*, 24:378–82.
https://doi.org/10.1159/000129231.

151. Sing SL, An J, Yeong WY, *et al*., 2016, Laser and Electron-beam Powder-bed Additive Manufacturing of Metallic Implants: A Review on Processes, Materials and Designs. *J Orthop Res*, 34:369–85.
https://doi.org/10.1002/jor.23075.